A review of major non-sulfide zinc deposits in Iran

Sajjad Maghfouri, Mohammad Reza Hosseinzadeh, Abdorrahman Rajabi, Flavien Choulet

▶ **To cite this version:**

Sajjad Maghfouri, Mohammad Reza Hosseinzadeh, Abdorrahman Rajabi, Flavien Choulet. A review of major non-sulfide zinc deposits in Iran. Geoscience Frontiers, 2017, 9, pp.249 - 272. 10.1016/j.gsf.2017.04.003 . insu-02538150

HAL Id: insu-02538150
https://insu.hal.science/insu-02538150

Submitted on 10 Mar 2021

HAL is a multi-disciplinary open access archive for the deposit and dissemination of scientific research documents, whether they are published or not. The documents may come from teaching and research institutions in France or abroad, or from public or private research centers.

L'archive ouverte pluridisciplinaire **HAL**, est destinée au dépôt et à la diffusion de documents scientifiques de niveau recherche, publiés ou non, émanant des établissements d'enseignement et de recherche français ou étrangers, des laboratoires publics ou privés.

Distributed under a Creative Commons Attribution - NoDerivatives 4.0 International License

Geoscience Frontiers 9 (2018) 249–272

HOSTED BY

Contents lists available at ScienceDirect

China University of Geosciences (Beijing)

Geoscience Frontiers

journal homepage: www.elsevier.com/locate/gsf

Research Paper

A review of major non-sulfide zinc deposits in Iran

Sajjad Maghfouri [a], Mohammad Reza Hosseinzadeh [a,*], Abdorrahman Rajabi [b], Flavien Choulet [c]

[a] Department of Earth Sciences, Faculty of Natural Sciences, University of Tabriz, Tabriz, Iran
[b] Department of Earth Sciences, University of Birjand, Birjand, Iran
[c] Chrono-Environnement, Université de Franche-Comté/CNRS, 25030 Besançon Cedex, France

ARTICLE INFO

Article history:
Received 6 January 2017
Received in revised form
27 March 2017
Accepted 5 April 2017
Available online 22 April 2017
Handling Editor: C. Spencer

Keywords:
Zinc-lead deposits
Supergene
Non-sulfide Zn minerals
Hemimorphite
Smithsonite
Hydrozincite

ABSTRACT

The numerous non-sulfide zinc ore deposits were the historical basis for the development of zinc mining in Iran. They include the Mehdiabad, Irankouh and Angouran world-class deposits, as well as the Zarigan and Haft-har deposits. These deposits were formed by supergene oxidation of primary sulfide minerals during the complex interplay of tectonic uplift, karst development, changes in the level of the water table, and weathering. Zn (Pb) carbonates, Zn-hydrosilicates and associated hydrated phases directly replace the primary ore bodies or fill cavities along fractures related to uplift tectonics. Direct replacement of primary sulfides is accompanied by distal precipitation of zinc non-sulfide minerals in cavities or internal sediments filling. The mineralogy of the non-sulfide mineralization in all six deposits is generally complex and consists of smithsonite, hydrozincite, and hemimorphite as the main economic minerals, accompanied by iron and manganese oxy-hydroxides and residual clays. Commonly, non-sulfide minerals in these deposits consist of two types of ore: red zinc ore (RZO), rich in Zn, Fe, Pb-(As) and white zinc ore (WZO), typically with very high zinc grades but low concentrations of iron and lead. Typical minerals of the RZO are Fe-oxyhydroxides, goethite, hematite, hemimorphite, smithsonite and/or hydrozincite and cerussite. Common minerals of the WZO are smithsonite or hydrozincite and only minor amounts of Fe-oxyhydroxides and hemimorphite.

© 2017, China University of Geosciences (Beijing) and Peking University. Production and hosting by Elsevier B.V. This is an open access article under the CC BY-NC-ND license (http://creativecommons.org/licenses/by-nc-nd/4.0/).

1. Introduction

"Non-sulfide" is a term, which comprises a series of oxidized Zn−(Pb) ore minerals, mainly considered as related to weathering of Zn (Pb) sulfide concentrations. These deposits may result from the supergene evolution of primary sulfide deposits such as Mississippi Valley-type (MVT), carbonate replacement, sedimentary exhalative (SEDEX), Irish type, veins and less commonly skarns (Heyl and Bozion, 1962; Hitzman et al., 2003). They can also be due to hypogene processes: (1) structurally controlled replacement deposits (Appold and Monteiro, 2009; Borg, 2009; Slezak et al., 2014), (2) stratiform lenses in highly metamorphosed terrains (Brugger et al., 2003; Peck et al., 2009) or (3) hydrothermal overprints of sulfide deposits (Boni et al., 2007; Boni, 2014). In the case of supergene processes, subtypes have been distinguished, including direct replacement deposits and wall-rock replacement deposits (Heyl and Bozion, 1962; Hitzman et al., 2003; Borg, 2015).

Direct replacement non-sulfide deposits, are characterized by local trapping of base metals liberated by sulfide dissolution with a very limited transport from the original protore zone. They usually display a 'red ore', that commonly consist of iron (hydr-) oxides (mainly goethite and hematite) associated with hemimorphite, smithsonite, hydrozincite and cerussite. Direct replacement non-sulfide deposits typically contain >20% Zn, >7% Fe and display high Pb ± As contents and commonly preserved sulfide minerals like galena, sphalerite, or pyrite (Reichert and Borg, 2008; Reichert, 2009).

Wall-rock replacement mineralization, also known as 'white ore' is characterized by the leaching and the transport of metals by percolating waters due to the groundwater/geochemical gradient (primary ore) (Heyl and Bozion, 1962; Hitzman et al., 2003). Wall-rock replacement deposits consist of smithsonite, hydrozincite and minor iron oxides, and contain <40% Zn, <7% Fe and very low concentrations of Pb (Boni et al., 2007; Reichert and Borg, 2008;

* Corresponding author.
E-mail address: mr-hosseinzadeh@tabrizu.ac.ir (M.R. Hosseinzadeh).
Peer-review under responsibility of China University of Geosciences (Beijing).

http://dx.doi.org/10.1016/j.gsf.2017.04.003
1674-9871/© 2017, China University of Geosciences (Beijing) and Peking University. Production and hosting by Elsevier B.V. This is an open access article under the CC BY-NC-ND license (http://creativecommons.org/licenses/by-nc-nd/4.0/).

Reichert, 2009; Boni and Mondillo, 2015). They may occur at the vicinity of the protore or up to several hundred metres away (Heyl and Bozion, 1962; Hitzman et al., 2003; Reichert and Borg, 2008; Reichert, 2009). As they are commonly richer in Zn and poorer in Pb and Fe (Reichert, 2009).

Despite the widespread occurrence of surficial zinc oxides in gossans and soils (e.g. Jacquat et al., 2009), economic non-sulfide deposits are far less common than sulfide deposits. Non-sulfide deposits have experienced a significant revival over the recent years, as a consequence of new developments in hydrometallurgical acid leaching, solvent extraction, and electrowinning techniques (Choulet et al., 2013). The non-sulfide Zn ore, called "calamine" by the miners includes a mixture of smithsonite, hemimorphite, hydrozincite locally associated with Fe-oxyhydroxides and clays.

The economic value of zinc non-sulfide ores is strictly dependent on the nature of the ore and gangue minerals. Host-rock composition may have significantly influenced the mineralogy (and by extension processing) of ores in these deposits. Since the differences in dissolution rates of the zinc minerals may have strong implications for the production strategies and metallurgical requirements, a detailed mineralogical and petrographic study, in the early phases of an exploration process, is required for this kind of ores, even more than in the case of sulfide deposits.

Scientific research, resulting from the economic interest shown by many mining companies in this style of mineralization, has focused on several potentially economic "Non-sulfide" deposits (e.g., Skorpion, Namibia: Borg and Kärner, 2001; Borg et al., 2003; Shaimerden, Kazakhstan: Boland et al., 2003; Vazante, Brazil: Monteiro et al., 1999; Beltana, Australia: Muller, 1972; Brugger et al., 2001; Hitzman, 2001; Groves and Carman, 2003; Hitzman et al., 2003; Angouran, Irankouh and Mehdiabad, Iran: Daliran, 2003; Daliran and Borg, 2004; Reichert, 2007; Reichert and Borg, 2008; Daliran et al., 2009).

Iran possesses a large range of Zn–Pb deposits including SEDEX, Irish-type and MVT that occur in carbonate and siliciclastic rocks (Rajabi et al., 2012). There are more than 350 Zn–Pb deposits and occurrences in Iran, including world-class deposits such as Angouran, Mehdiabad and Irankouh (Borg, 2005; Rajabi et al., 2012) (Fig. 1). Only a few of them, however, have actually been explored

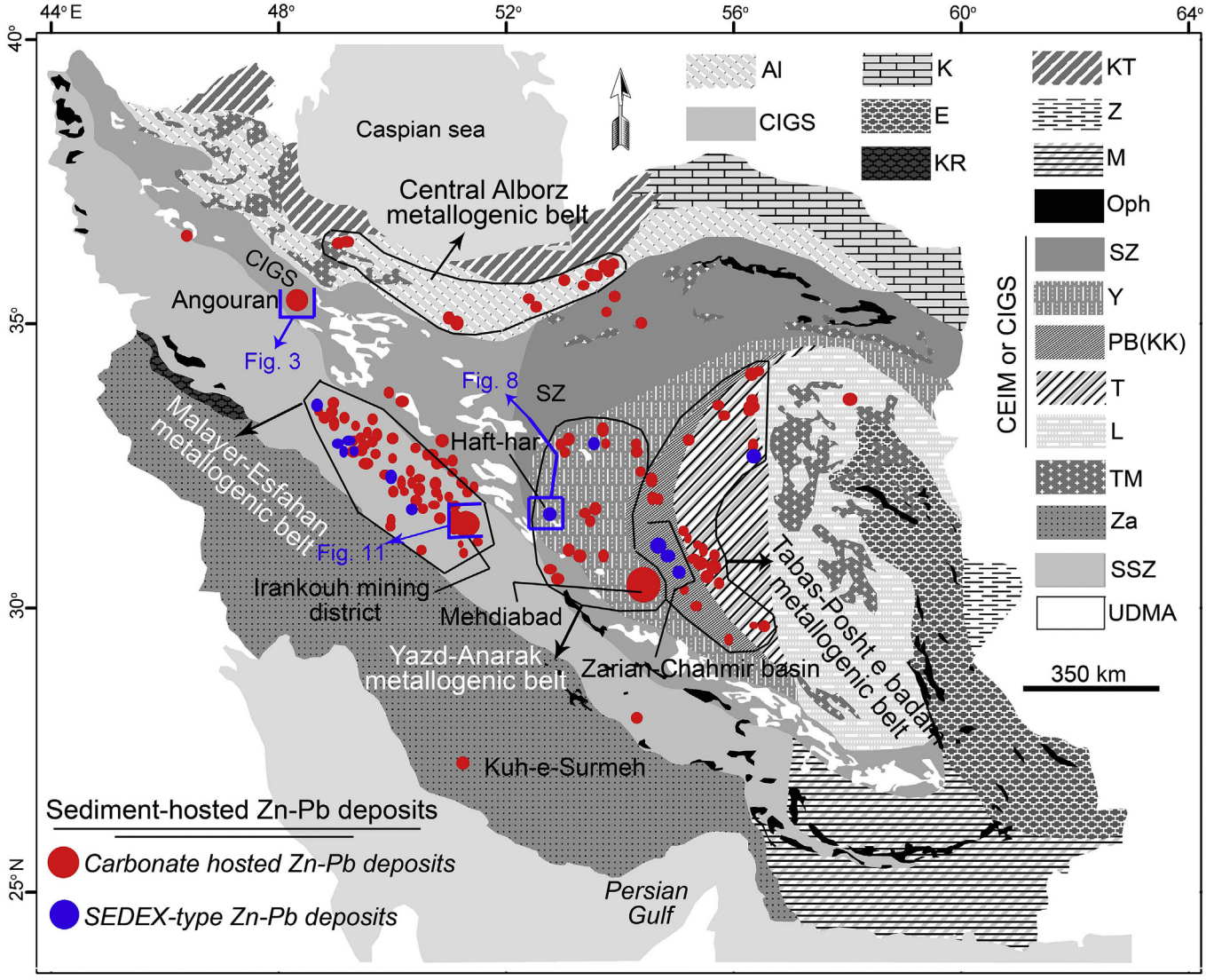

Figure 1. Distribution map of sediment hosted Zn–Pb deposits according to the type of ore deposits in the main tectonic elements of Iran. Al, Alborz zone; CIGS, Central Iranian geological and structural gradual zone; E, East Iran ranges; K, Kopeh-Dagh; KR, Kermanshah Radiolarites subzone; KT, Khazar-Talesh-Ziveh structural zone; L, Lut block; M, Makran zone; Oph, ophiolite belts; PB, Posht-e-Badam block; SSZ, Sanandaj-Sirjan zone; T, Tabas block; TM, tertiary magmatic rocks; UDMA, Urumieh-Dokhtar magmatic arc; Y, Yazd block; Z, Zabol area; Za, Zagros ranges. Tectonic and structural map of Iran modified after Alavi (1996) and Aghanabati (1998, 2004).

and exploited. The largest of these deposits is the Mehdiabad deposit. This study focuses on six ore deposits throughout the Iran (Table 1). These deposits include Angouran, Irankouh, Mehdiabad, Kuh-e-Surmeh, Zarigan and Haft-har (Fig. 1 and Table 1).

2. Methodology

The available information (as far as possible) on the Zn–Pb deposits of Iran has been incorporated into a sedimentary structural map of Iran and integrated into a comprehensive GIS database. Most of the data were derived from the inventories of the Geological Survey of Iran and from published and unpublished data of numerous source papers cited in the references. Because of the large number of nonsulfide Zn–Pb deposits and occurrences, and the lack of information about most of them, we tried to avoid unreliable occurrences and removed very small occurrences from the database. So, the authors have visited the six major nonsulfide Zn–Pb deposits and studied different geological characteristics of these deposits. Also we present field observations of macrostructures and try to decipher the relationships between the protore, the non-sulfide zone, and the host rocks.

3. Zinc–lead deposits in Iran

Most Zn–Pb deposits occur within continental blocks, which are key structures in the evolution of the Palaeo-Tethys and Neo-Tethys oceans. There is no information about the age of these deposits, but host rocks range from Devonian to Late Cretaceous. Iran is a part of the Tethyan Belt and, hence, the numerous mineral deposits are related to the tectonic evolution of the Tethys Ocean. Although Iran is well known for porphyry and epithermal (Cu–Au) deposits (Aghazadeh et al., 2015), it also hosts a range of significant Zn–Pb deposits (Borg, 2005). They belong to the Tethyan Metallogenic Belt, similarly to those of China and Turkey (Reynolds and Large, 2010). Fig. 1 shows the distribution of the diversely aged sediment-hosted Zn–Pb deposits in Iran, which include both primary sulfide and secondary non-sulfide concentrations (Borg, 2005; Rajabi et al., 2012).

3.1. Sedimentary exhalative massive sulfide or SEDEX deposits

The most important SEDEX Zn–Pb deposits of Iran occur in the NW, Central and SE parts of the Zarigan–Chahmir basin in the Poshteh-Badam and Yazd block (YB) and in the Malayer-Esfahan metallogenic belt (MEMB) (Fig. 1). The Koushk, Zarigan, Chahmir and Haft-har Zn–Pb deposits are the major ones (Rajabi et al., 2014). They commonly occur close to the intersection of syn-sedimentary faults (active throughout the sag-phase of the Zarigan–Chahmir basin evolution; Rajabi et al., 2012) and are hosted by sedimentary rocks deposited under anoxic conditions (Rajabi, 2012). Three major ore zone or facies are usually distinguished in the SEDEX Zn–Pb deposits in Iran (Rajabi, 2012; Rajabi et al., 2012): (1) massive sulfide ore or vent-complex, (2) stockwork or feeder zone, and (3) stratiform-bedded ore, which include exhalites and lenses of pyrite, sphalerite and galena.

3.2. Carbonate hosted (CH) Zn–Pb deposits

Based on the age of their host rocks, two major groups of CH Zn–Pb deposits can be distinguished and linked to different tectonic events that affected the Iranian Plate. The first group includes the Permian–Triassic-hosted MVT deposits mainly in the Central Alborz and Tabas-Posht e Badam metallogenic belts, and in the northeastern margin of the Sanandaj–Sirjan zone (SSZ) (Fig. 1). The Triassic carbonate rocks also host numerous F-rich deposits,

Table 1
Main features of the most important non-sulfide deposits quoted in text.

Name	Location zone	Type of deposit	Host rocks	Host rock age	Supergene type	Oxidation age	Sulfide minerals	Oxide minerals	References
Mehdiabad	YAMB	SEDEX	Shale, siltstone and dolomite	Early Cretaceous	DR (WR)	Post-early Cretaceous	Sph, Gn, Py, Cpy, Cc	Hm, Sm, Hz, Cer, Fe-Mn oxide	Reichert (2007), Maghfouri et al. (2015) and Maghfouri (2017)
Irankouh	MEMB	Unknown - SEDEX (Gushfil and Tapeh-Sorkh)	Dolomite, shale, siltstone and tuff	Early Cretaceous	DR (WR)	Post-early Cretaceous	Sph, Gn, Py, (Cpy)	Hm, Sm, Hz, Cer, Fe-oxide	Rastad (1981), Reichert (2007), Boviri and Rastad (2016) and Boveiri et al. (2017)
Kuh-e-Surmeh	Zagros zone	MVT	Dolomite and dolomitic limestone	Devonian–Early Permian	WR (DR)	Post-early Permian	Sph, Gn, (Py)	Sm (Cer, Hm, Hz)	Liaghat et al. (2000) and Reichert and Borg (2008)
Haft-har	YAMB	SEDEX	Shale, siltstone and tuff	Cambrian	DR	Post-Cambrian	Py, Sph, Gn	Cer, Hem, Fe-oxide (Sm, Ang)	Movahednia (2014)
Zarigan	PB	SEDEX	Siltstone and silty limestone	Early Cambrian	DR	Post-early Cambrian	Py, Sph, Gn	Fe-oxide, Cer, Sm (Hm, Ang)	Rajabi (2012)
Angouran	SSZ	Unknown	Marble and schist	Neoproterozoic–Early Cambrian	DR (WR)	Post-early Cambrian	Sph, Gn, Py, (Cpy)	Sm, Hz, (Hm, Cer, Fe-oxide)	Daliran (2003), Daliran and Borg (2004), Annels (2005), Gilg et al. (2006), Boni et al. (2007), Daliran et al. (2009) and Daliran et al. (2013)

Zones: YAMB = Yazd-Anarak metallogenic belt; MEMB = Malayer-Esfahan metallogenic belt; SSZ = Sanandaj-Sirjan zone; PB = Posht-e-Badam Block.
Type of deposits: SEDEX = sedimentary exhalative massive sulfide deposit; MVT = Mississippi Valley-type deposit.
Supergene deposit types: DR = direct replacement; WR = wall-rock replacement.
Minerals: Cer = cerussite; Hm = hemimorphite; Hz = hydrozincite; Sm = smithsonite; Ang = anglesite; Py = pyrite; Sph = sphalerite; Gn = galena; Cpy = chalcopyrite; Cc = chalcocite.

marked by stratabound mineralization and veins of fluorite, barite with minor galena and sphalerite. The second group includes the Zn–Pb deposits hosted in the Cretaceous series, located in the Malayer-Esfahan and Yazd-Anarak metallogenic belts (YAMB), and to a lesser extent, in the Central Iranian Geological and Structural (CIGS) transition zone and in the Central Alborz metallogenic belt (AMB) (Fig. 1).

4. Supergene non-sulfide zinc-lead deposits in Iran

Iran exposes numerous non-sulfide zinc deposits, and several centers for zinc smelting and refining were established near the mining sites. Furthermore, there are additional non-economic resources in mine dumps, flotation tailings, and smelter residues. Although these can be quite substantial in areas of ancient mining (e.g., Angouran and Mehdiabad), they will not be discussed further in this paper. Most of the Iranian examples of non-sulfide zinc mineralization belong to the group I (classification of Large, 2001) calamine deposits, hosted by carbonate rocks.

Non-sulfides deposits of Iran widespread in the different tectonics blocks of Iran. The most important metallogenetic provinces for non-sulfide zinc mineralization are Central Iran, the Sanandaj–Sirjan zone, and the Alborz region (Fig. 1). The age of the host rocks ranges from Proterozoic to Tertiary. However, most of the host rocks are either Mesozoic or Cretaceous carbonates (Table 1). Only a few non-sulfide zinc deposits (Angouran, Irankouh, and Mehdiabad) are currently mined (Fig. 1). The giant Mehdiabad deposit is a special case, as both sulfide and non-sulfide ores are currently mined. In this paper we focus on the important non-sulfide deposits in Iran (Table 1).

4.1. Late Neoproterozoic–Early Paleozoic hosted non-sulfide deposits

4.1.1. The Angouran deposit

The Angouran Zn(–Pb–Ag) deposit is located in the western part of Zanjan Province, NW Iran (Fig. 1). This area belongs to the northwestern part of the Sanandaj-Sirjan Zone, a metamorphic belt related to the Zagros orogeny (Fig. 2).

The basement rocks at Angouran include imbricated thrust sheets of exhumed metamorphic rocks that consist of muscovite-, chlorite- and quartzite-schists with thin marble horizons and a discontinuous 50–100 m thick interval of meta-basic amphibolite schist (Daliran et al., 2013). Foliated pillow basalt and serpentinite bodies, which represent a mid-ocean ridge ophiolite assemblage are also present (Figs. 3 and 4) (Daliran et al., 2013). The footwall quartzite schist is equivalent to the Neoproterozoic Kahar Formation (Daliran et al., 2013). The U–Pb age of 511 Ma obtained by SHRIMP-dating on inherited cores of the zircon in pillow basalts indicates that the basalts probably formed during the Cambrian (Daliran et al., 2013). The 94 Ma U–Pb age for the rim of these zircon grains is interpreted as a metamorphic overgrowth during the Alpine orogeny (Daliran et al., 2009). The marble unit (Angouran Marble) was thrusted onto the schists (Fig. 4) and contains discontinuous dolomitic horizons with supergene dissolution cavities, locally. The age of the marble unit is also Neoproterozoic to Early Cambrian based on the microfauna content (e.g. Siphogonuchites triangularis; Hamdi, 1995) (Fig. 4).

The host rocks at Angouran are part of a 70 km × 30 km block of stacked thrust sheets comprising marble, schists and ultrabasic basement rocks (Fig. 3) (Daliran et al., 2013). Footwall schists within the mine sequence are intensely deformed and comprise whitish to light green quartz-sericite schist and pale orange calcareous schist with intercalations of quartzite and subordinate muscovite-, chlorite-, epidote- and biotite-schist with thin marble bands (Fig. 4) (Daliran et al., 2009, 2013). Toward the north, the schist sequence is underlain by a discontinuous interval of 50–100 m of metamorphosed basic and ultrabasic rocks including pillow basalt, amphibolite, metabasalt and serpentinite. The hanging-wall consists of a 50–300 m thick marble unit (Angouran Marble) (Fig. 4) (Daliran et al., 2013). The marble is thick to medium bedded, light to medium gray with thin, discontinuous dark laminae (carbonaceous material) and subordinate dolomitic intercalations.

Figure 2. View of the Angouran open pit; the brown color correspond to the non-sulfide ore. Host rock of the non-sulfide ore is marble.

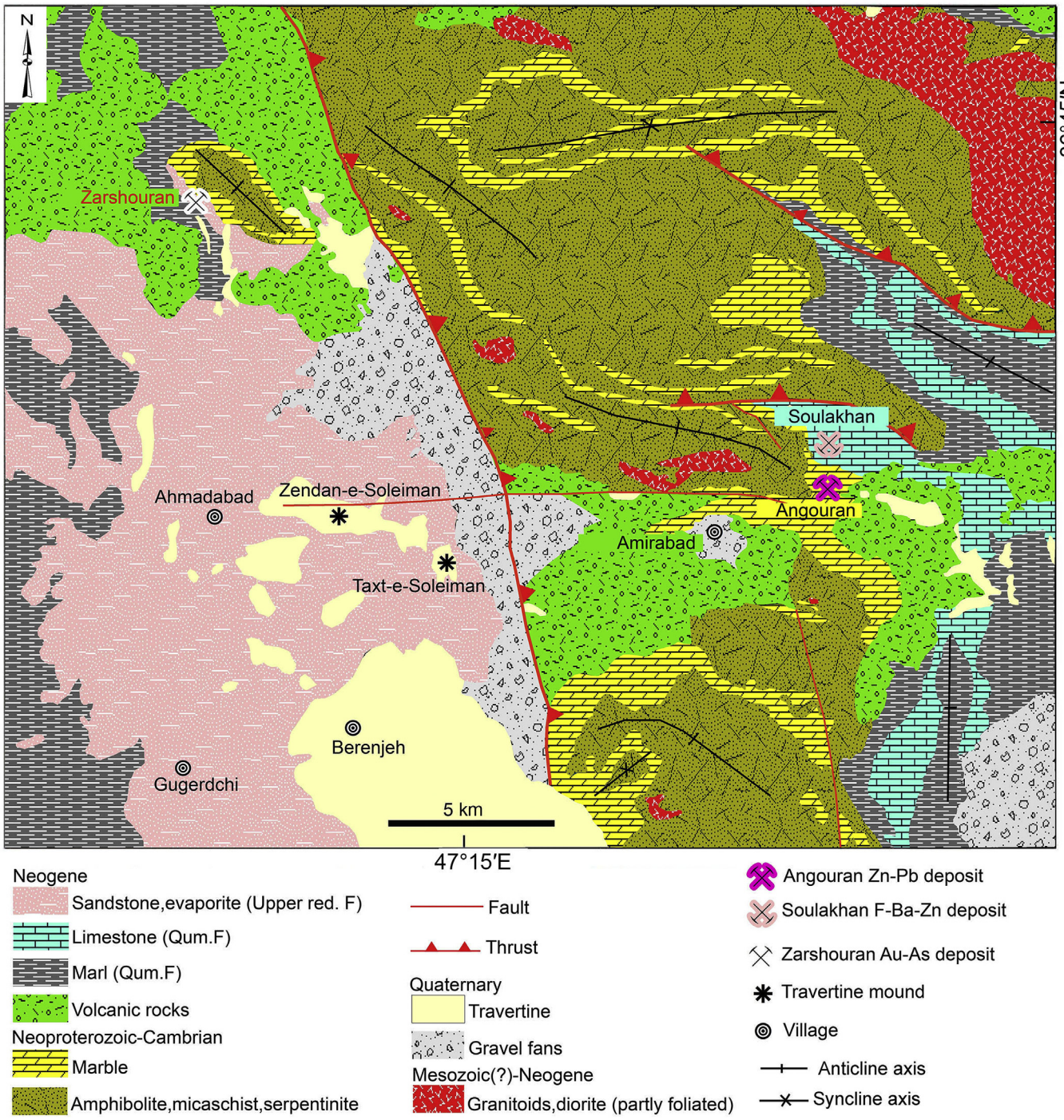

Figure 3. Schematic regional geological map of the Angouran area, NW Iran (after Babakhani and Ghalamghash, 1990).

Recent mining (Fig. 3) began after the rediscovery of the Zn ore in cerussite-bearing gossans, in surface outcrops and dissolution cavities in the hanging-wall marble in 1922. The ore reserve in 2001 was 4 Mt sulfide ore (40.4% Zn, 1.9% Pb) and 18.23 Mt carbonate ore (28.1% Zn, 4.4% Pb, and 110 g/t Ag; Pride and Salehi, 2003).

The orebody exhibits a vertical zonation with (1) an underlying Zn-rich, hypogene, sulfide ore, and a mixed sulfide–carbonate ore at the bottom and, (2) a carbonate ore at the top. The deposit formed at a lithological boundary, which comprises a thrust contact between the footwall schists and the hanging-wall marbles (Figs. 3 and 4). The ore zone at Angouran displays a complex geometry. The hypogene sulfide deposit, which has been oxidized to form a significant non-sulfide orebody, mainly in the form of smithsonite, is located at the crest of an open anticline at the contact between Neoproterozoic to Cambrian footwall micaschists and hanging wall marbles (Boni et al., 2007). The dimensions of the mineralized zone are ca. 600 m in length (along the N–S axis) and 200 to 400 m in width. The orebodies are delimited by two

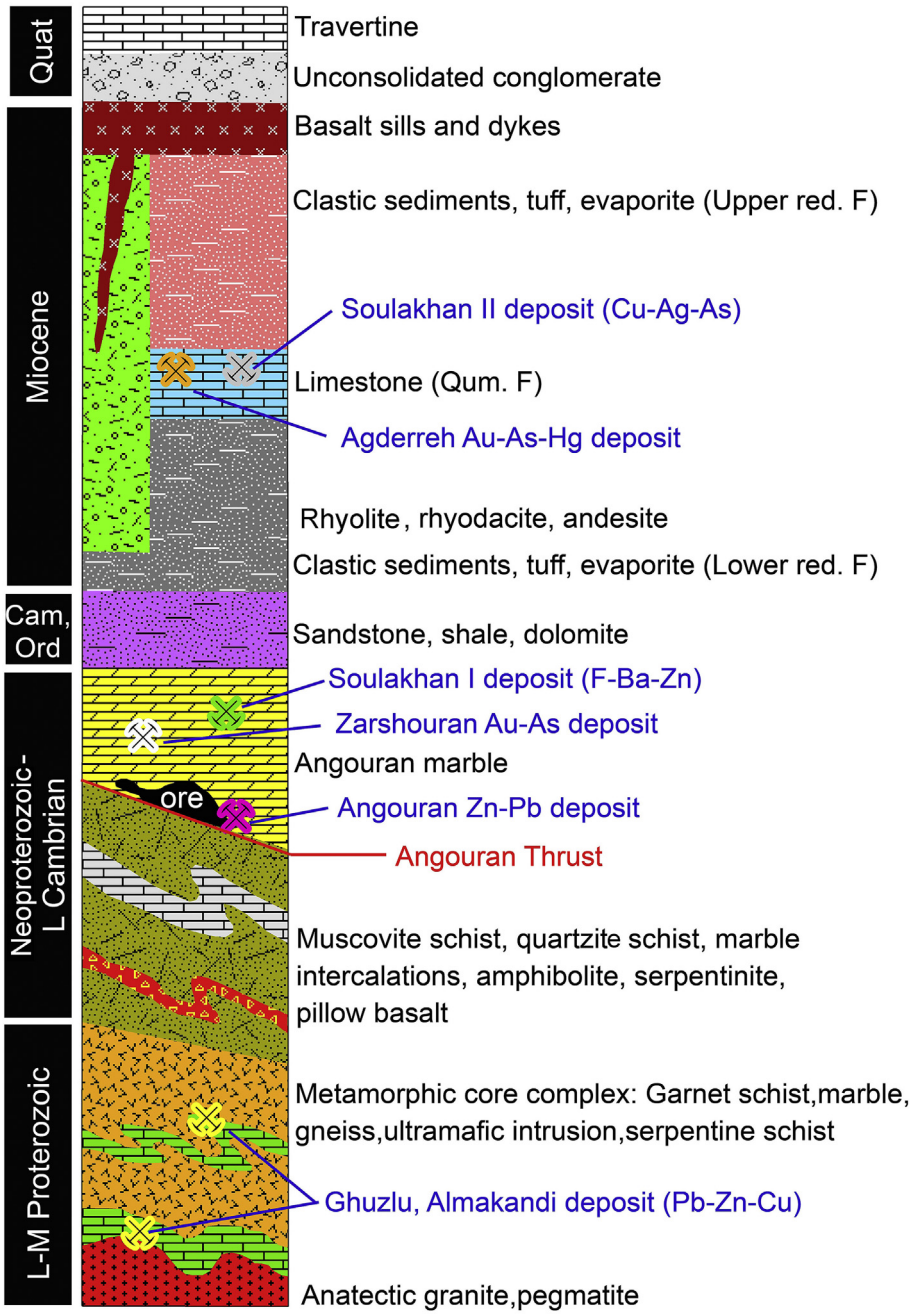

Figure 4. Generalized schematic columnar section of the Angouran area, with the main ore-bearing strata (modified after Daliran et al., 2013).

major NNW–SSE and NW–SE trending faults and a third NE–SW fault trending (Fig. 3). The thickness of the zinc carbonate ore zone may reach up to 200 m; this ore zone occurs in the hanging-wall marbles and overlies a tabular sulfide orebody (Boni et al., 2007; Daliran et al., 2013; Boni and Mondillo, 2015). Smaller bodies of mixed sulfide and carbonate ore occur at the contact between sulfide and non-sulfide zones, as well as within the non-sulfide ores. Both ore types also fill a wide variety of breccias, especially along the three main fault zones that are laterally controlling the deposit.

Previous genetic models proposed for the Angouran sulfide deposit include a wide range of models (SEDEX and VMS) and ages (Proterozoic to Mesozoic) (e.g., Gazanfari, 1991; Ghorbani, 1999; Annels, 2005). These essentially syngenetic models were challenged by more recent studies that document an epigenetic model of formation for the sulfide ore (e.g., Daliran, 2003; Daliran and Borg, 2004; Gilg et al., 2006; Boni et al., 2007; Daliran et al., 2009). Hirayama (1968), however, recognized the unmetamorphosed nature of the sphalerite ore and concluded that the mineralization was post-metamorphic.

The mineralogy of the supergene and hypogene parts of the deposit mainly consists of smithsonite (Fig. 5), arsenopyrite, galena, sphalerite, pyrite, greenockite, Co-arsenopyrite, cerussite, pyromorphite, Zn-arsenates, Co–Ni-arsenates, Pb–Mn-(hydr) oxides, hemimorphite, litharge, several clay minerals, and apatite (Fig. 5) (Boni et al., 2007). The genesis of the Angouran Zn carbonate ores is

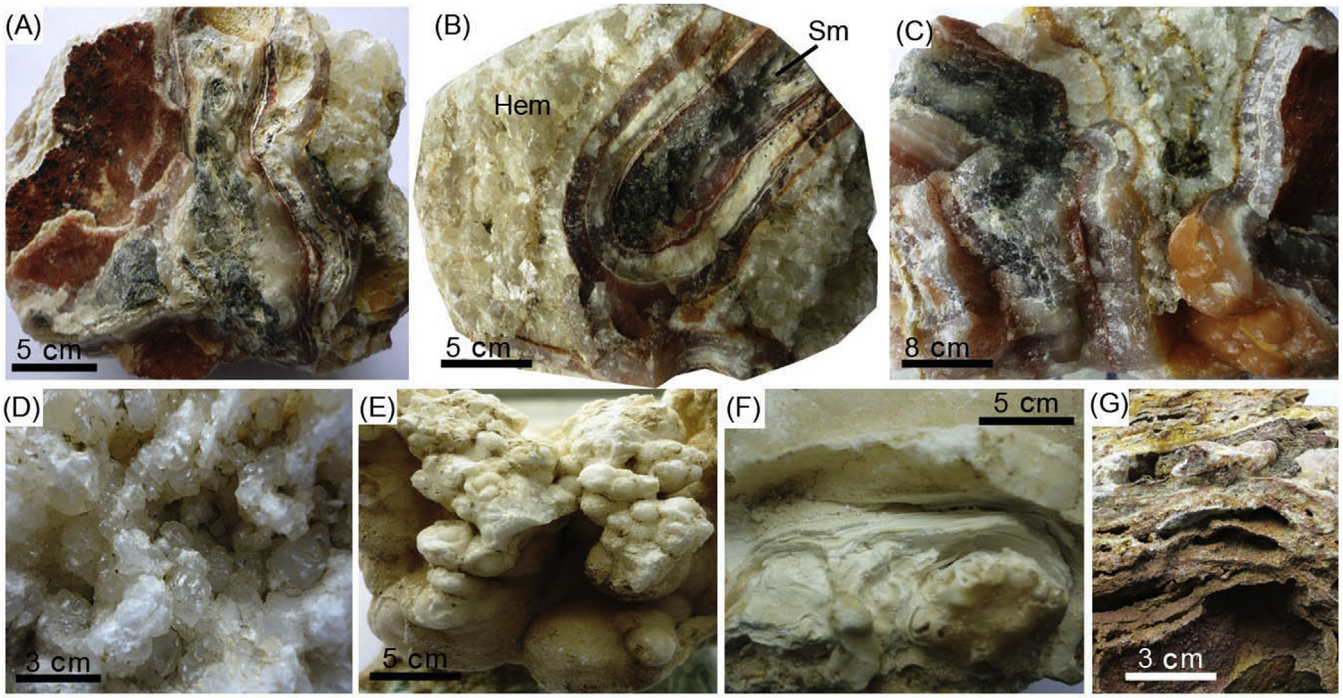

Figure 5. Images of supergene non-sulfide zinc minerals from the Angouran deposit. (A) Colloform smithsonite; (B) hemimorphite (Hem) crystals around a core of colloform smithsonite (Sm); (C) concretionary smithsonite; (D) crystalline hemimorphite; (E) botryoidal smithsonite filling vug; (F) white ore sample made of hydrozincite [$Zn_5(CO_3)_2(OH)_6$]; (G) aggregate of goethite, hematite and smithsonite.

distinct from that of other "classical" non-sulfide Zn deposits that formed entirely by supergene processes, as demonstrated also by carbon and oxygen isotope geochemistry (Daliran, 2003; Daliran and Borg, 2004; Daliran et al., 2009; Boni and Mondillo, 2015). Therefore, non-sulfide mineralization at Angouran is interpreted to be the result of during two successive stages, following an early generation of hypogene sulfide minerals. The first, main stage of Zn carbonates (stage I carbonate ore) is associated with both preexisting and subordinate newly formed sulfides, whereas the second stage is characterized by supergene carbonates (Zn and minor Pb), associated with oxides and hydroxides (stage II carbonate ore) (Boni et al., 2007; Daliran et al., 2013; Boni and Mondillo, 2015).

4.1.2. Zarigan SEDEX-type deposit

The central lithotectonic domain of the Posht-e-Badam Block, within the Central Iranian microcontinent, contains the oldest (Late Neoproterozoic) basement of Iran (Rajabi et al., 2012). The Zarigan–Chahmir basin is located in the southern section of this lithotectonic domain (Fig. 1) and hosts abundant mineral deposits, especially iron oxide–apatite (IOA) deposits, Fe–Mn exhalative deposits, and sedimentary exhalative (SEDEX) Zn–Pb deposits (Rajabi et al., 2012). The economically most important SEDEX Zn–Pb deposits of this basin include the Koushk, the Chahmir and the Zarigan deposits (Rajabi et al., 2012).

The Zarigan Zn–Pb deposit is hosted within the upper part of the Early Cambrian Volcano-Sedimentary Sequence (ECVSS), in the northern part of the Zarigan–Chahmir basin (Fig. 6). Two sequences can be distinguished (Fig. 6): (I) a lower volcano-sedimentary (syn-rift) sequence well exposed in the Narigan, Esfordi, Lakeh-Siyah and Zarigan areas, which comprises gray basic coarse-grained clastic rocks, various pyroclastic rocks and bimodal volcanic rocks; and (II) the upper sedimentary sequence (corresponding to the post-rift sag-phase), including calcareous shales, siltstones and carbonates with minor tuffaceous rocks. The intercalated calcareous black siltstone of the post-rift sequence hosts the Zarigan SEDEX Zn–Pb mineralization, typically in its middle part (Fig. 6A).

The Zarigan deposit differs from other SEDEX deposits in the basin by its intensive weathering and the development of an oxidized Pb(–Zn) ore zone (Fig. 6). Ore minerals include cerussite, anglesite associated with abundant Fe-(hydr) oxides and minor pyrite, sphalerite and galena (Fig. 7 and Table 1). Therefore, red zinc ore (RZO) is dominant in the Zarigan SEDEX type deposit. Exploration of the sulfide ore is in early stages. Based on the previous mining activities (from 1957 to 1977), the primary sulfide ore reserve is estimated to be about 18–20 Mt, with 10 Mt of oxidized ore (Simiran Mining Co.). The host rocks at Zarigan include black siltstone and minor silty limestone (Fig. 6). In addition to some relict bands of sulfide minerals within the oxidized ore zone, laminated-disseminated sulfide minerals occur within the host rock (Fig. 7). Similar to the Lady Loretta deposit in Australia (Hancock and Purvis, 1990), zinc has been completely removed from the gossan cap and the oxidized zone (Figs. 6 and 7). The Zarigan deposit occurs as a single, wedge-shaped ore body within the host rock. The northern part of the deposit displays a stratabound geometry, but toward the south, as thickness decreases, the mineralization becomes stratiform and concordant with the host sedimentary rocks. Based on crosscutting relationships, mineralogy and texture of sulfide and non-sulfide mineralization, three major ore facies types can be distinguished, from proximal to distal relative to the syn-sedimentary Zarigan Fault (Rajabi, 2012): (1) a complex stratabound oxide ore, formed by replacement, open space filling and vein and veinlets of cerussite, anglesite, hematite, goethite with minor smithsonite, hemimorphite, pyrite and galena; (2) a bedded stratiform oxide ore, including laminated cerussite and hematite (relict textures of primary laminated sulfides) with disseminated pyrite and galena (Fig. 7A and B); and (3) a bedded stratiform sulfide ore, consisting of a banded body of

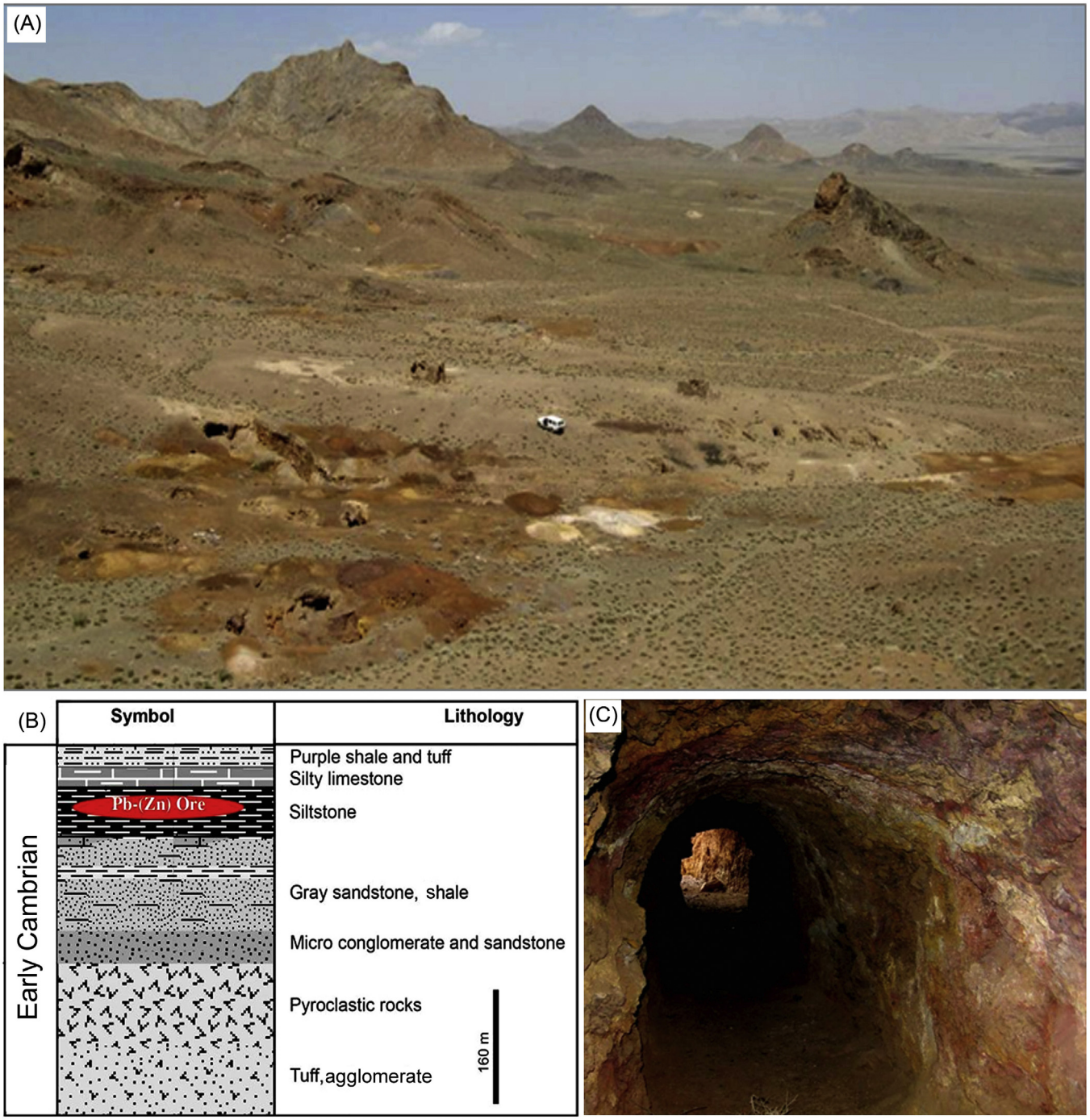

Figure 6. (A) General view of the mineralized area in the Zarigan. (B) Generalized lithostratigraphic columnar section of the Zarigan deposit, Zn–Pb-bearing horizons is located within the Early Cambrian sequence (Rajabi et al., 2012). (C) The main exposure at the Zarigan deposit in the old tunnel, an example of a siltstone-hosted non-sulfide base metal deposit with an iron-rich gossan component (Rajabi et al., 2012).

cerussite, anglesite, smithsonite, hemimorphite, pyrite and sphalerite with disseminated galena. In addition, banded chert facies, consisting of chert beds with barite and disseminated pyrite, overlies these ore facies types. These ore facies types and deposit geometry, together with the presence of a syn-sedimentary fault adjacent to the deposit, have led us to classify the Zarigan deposit as a vent-proximal (Selwyn-type) SEDEX deposit, equivalent to the Koushk and the Chahmir deposits (Rajabi, 2012).

4.1.3. Haft-har SEDEX-type deposit

The Haft-har Zn–Pb deposit, located about 260 km to the NW of Mehdiabad deposit, is hosted within the middle part of the Cambrian series of the Yazd block in Central Iran (Fig. 8). The footwall rocks are gray shales with interbedded sandstone (litharenite) and sandy volcaniclastic rocks. The ore-bearing zone occurs within the Haft-har unit, which consists of carbonaceous, fine-grained black siltstone and shale with intercalated volcaniclastic sandstone (Fig. 8). Limestone and massive cherty dolomite of the

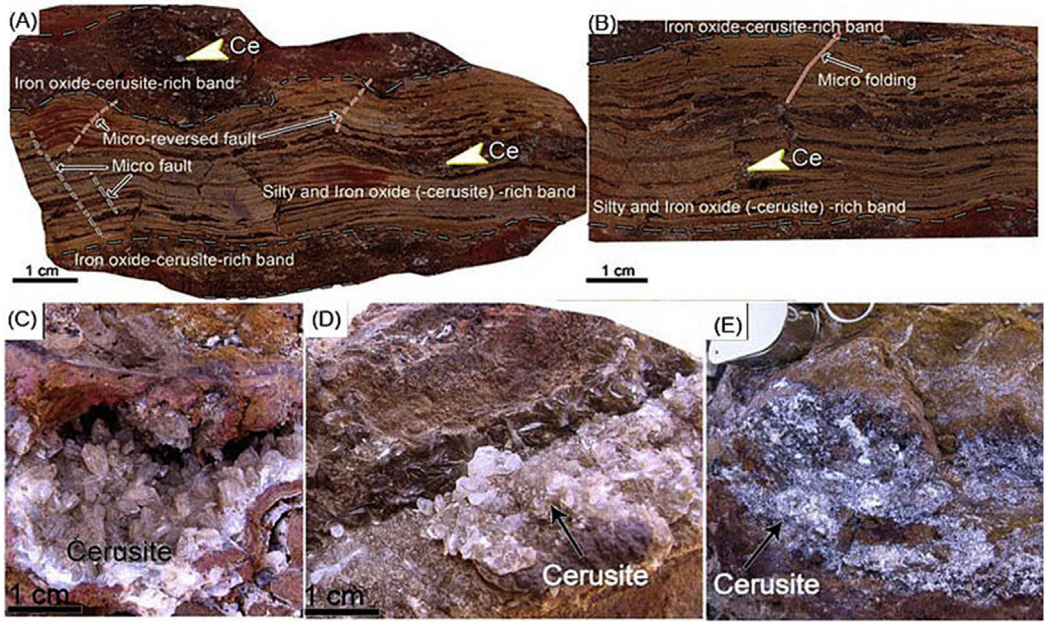

Figure 7. Images of supergene non-sulfide zinc samples in Zarigan deposit (Rajabi et al., 2012). (A and B) Hand sample of bedded non-sulfide ore, which have been completely oxidized to goethite, hematite and cerussite; (C) coarsely crystalline white-tan cerussite filling vugs in hematitic siltstone; (D and E) crystalline cerussite covering iron oxides.

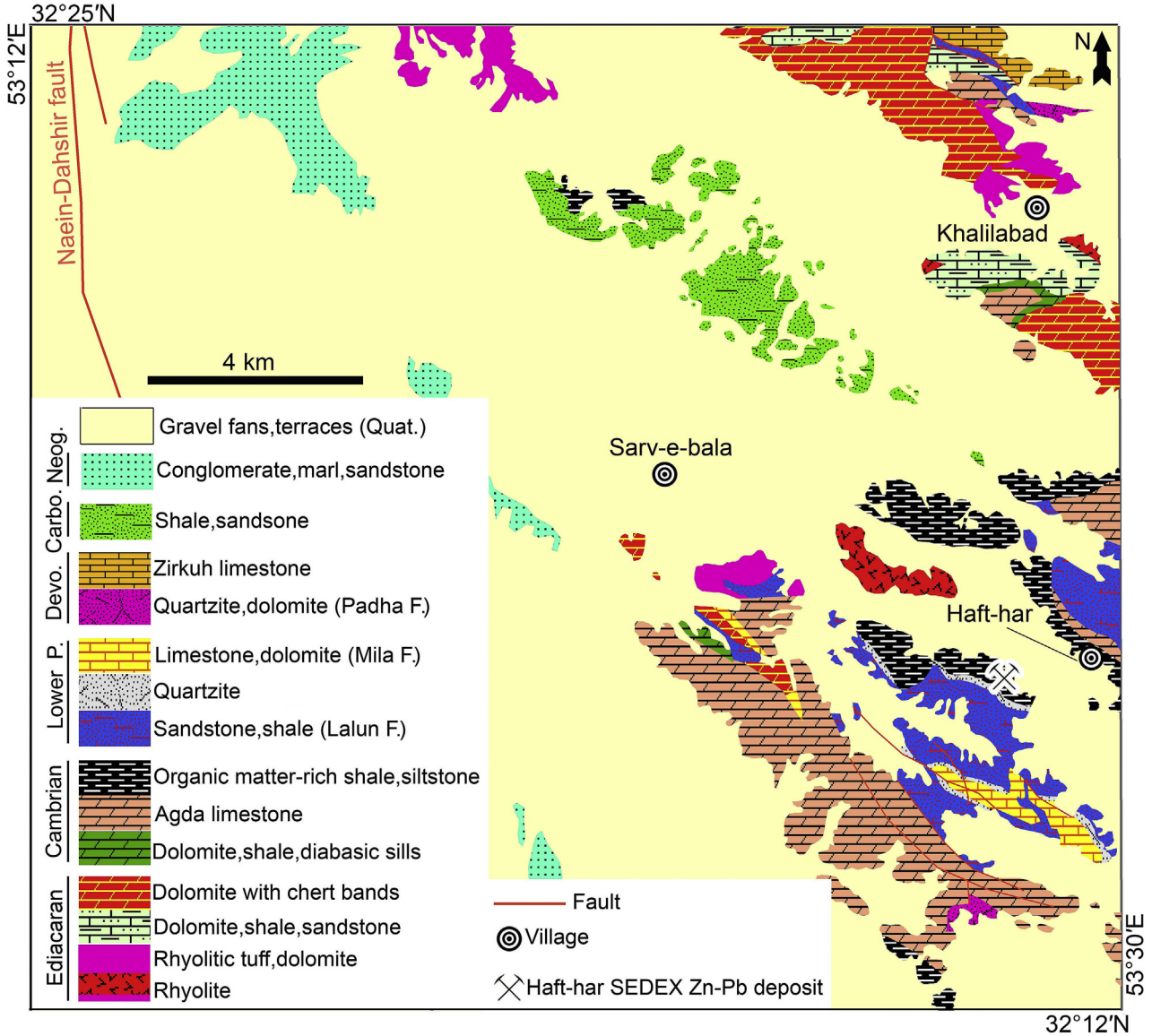

Figure 8. Simplified geological map of the Haft-har area in the Yazd block, showing the location of Haft-har SEDEX deposits within this map.

Mila Formation with thrust fault cover the ore-bearing shale and siltstone in the Haft-har area (Fig. 9A).

The sulfide lens of the Haft-har deposit does not crop out at the surface; therefore, the geological setting of the deposit has been reconstructed from drill core logs and adits (Fig. 9). Sulfide mineralization occurs as a single wedge within the organic matter-rich siltstone and shale. The ore-bearing host rock is usually folded, whereas the more competent dolomite typically exhibits a brittle deformation resulting in extensive breccia zones cut by late calcite veins. The limestone of the Mila Formation in the vicinity of the ore body has developed a large karst system probably caused by sulfide oxidation in the vicinity. Evidence of remobilization includes the precipitation of secondary minerals along joints and fractures of the host rock (Fig. 9C). The potentially economic resource of Haft-har deposit mainly consists of non-sulfide Zn minerals, associated with abundant Fe-(hydr) oxides; this non-sulfide mineralogy results from weathering of presumed primary sulfide minerals (Fig. 9). The primary orebody is likely to have been deformed and oxidized during post-Cambrian episodes. Preliminary mineralogical studies have revealed that the main sulfide phases are sphalerite, pyrite and galena, and are accompanied by calcite, barite and quartz (Movahednia, 2014).

Non-sulfide mineralization at Haft-har mainly consists of Fe-(hydr) oxides, smithsonite and hemimorphite, with subordinate hydrozincite. Cerussite and anglesite also occur, generally associated with nodules and lenses of residual or supergene galena (Fig. 9). A complex association of Fe and Mn oxy-hydroxides, with a characteristic red-brown color (goethite, lepidocrocite, hematite), and residual clay minerals hosts the non-sulfide ore (Fig. 9). The ore grade of the non-sulfide zone is highly variable throughout the mining district, ranging from 8% to more than 30% in the areas where the alteration profile displays a total replacement of sulfide minerals by secondary carbonates. As the dominant sulfide ore is rich in pyrite, a red zinc ore was formed in this deposit. The non-sulfide ore is rich in Zn in the lower levels of the oxidation profile, whereas, near the surface (in the leaching zone), the ore grade is generally not economic. The mineralization is considered to be the result of in situ oxidation of the primary sulfide ore by meteoric fluids, with increased acidity owing to the dissolution of substantial amounts of pyrite. The dissolution was followed by a more or less total replacement of the sulfide minerals, as well as of parts of the host rocks, by secondary minerals. Subsequent remobilization and further deposition of secondary minerals within dissolution vugs and karst cavities locally represent the last stages of the deposit evolution.

4.1.4. *Kuh-e-Surmeh deposit*

The Kuh-e-Surmeh Zn–Pb deposit is the only mineralization occurring within the southern part of the Zagros ranges (Fig. 1) in the Firoozabad region. The total Zn:Pb ratio of the deposit is 3:1, with average ore grades around 19% Zn and 7% Pb; the orebody contains approximately 990,000 tons of pre-mining reserves (Liaghat et al., 2000). The stratigraphic sequence of the mine area (Fig. 10) begins with more than 1000 m of Ordovician sediments of the Zard-Kuh Formation, which are silty, micaceous, olive-green shales and associated fine-grained dark-brown sandstone

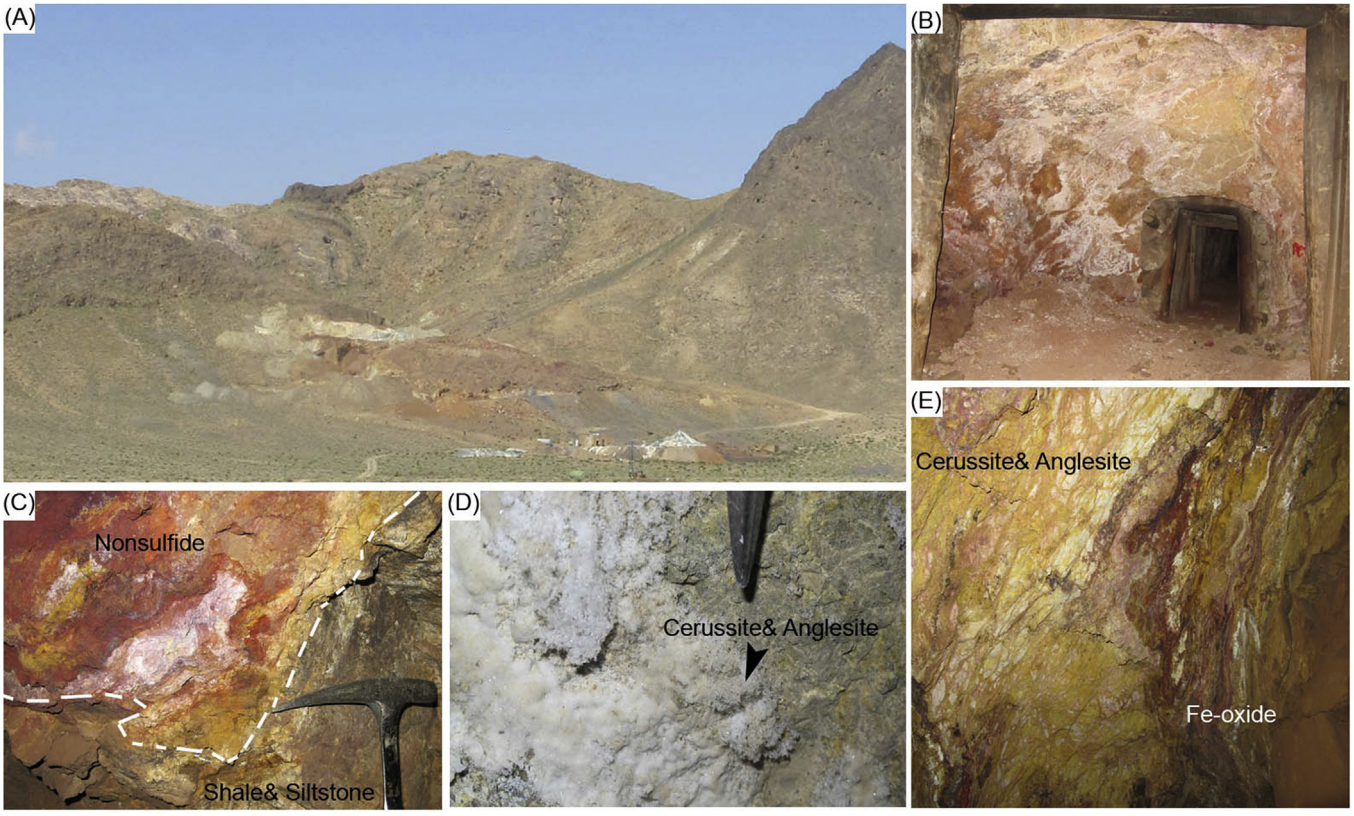

Figure 9. (A) General view of the Haft-har deposit. (B) Widespread non-sulfide ore (white) and Fe-oxide ore (red) forming the wall of underground tunnel. (C) Shale and siltstone host rocks overlain by iron oxide and a non-sulfide mineralization. (D) Crystalline white cerussite and anglesite coating the wall of tunnels. (E) Cerussite and associated to an iron oxidized facies.

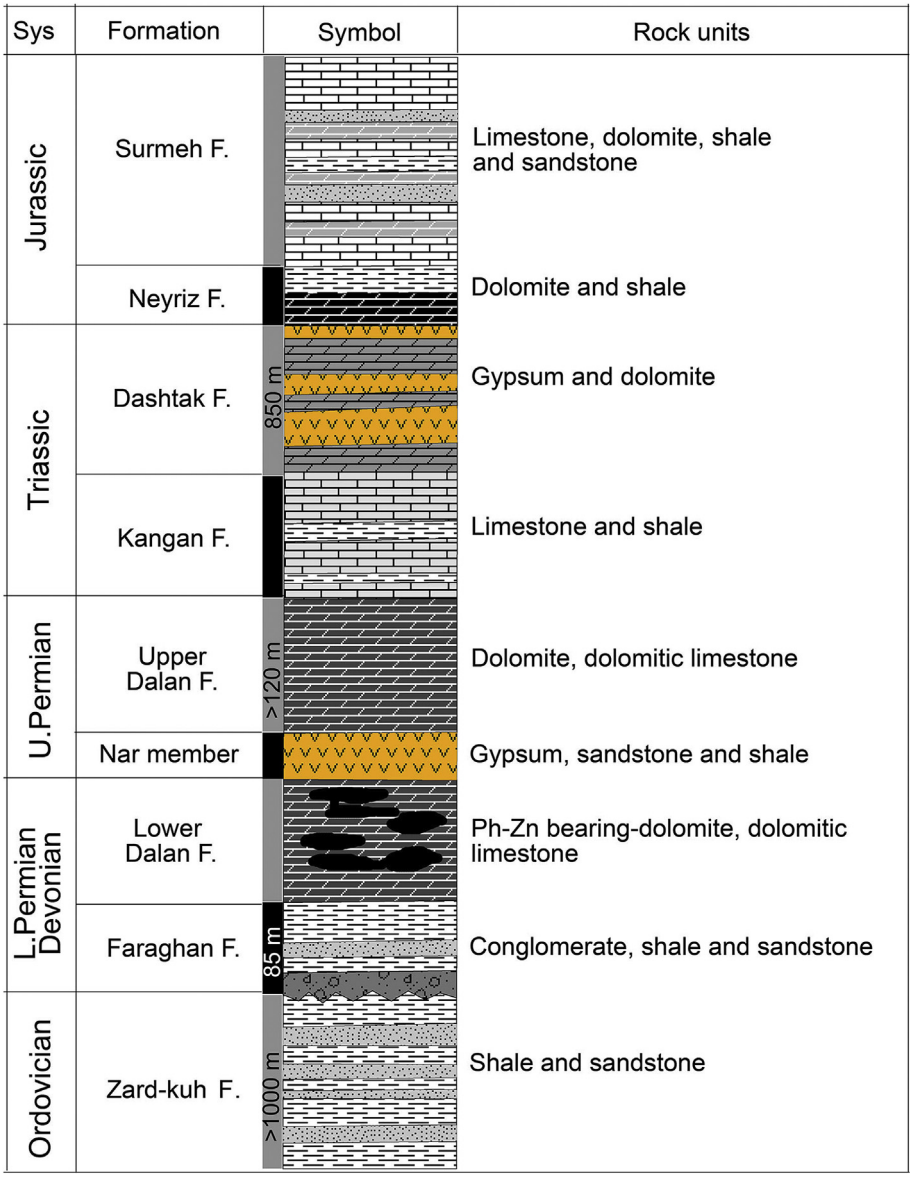

Figure 10. Regional stratigraphic sequence of the Kuh-e-Surmeh deposit. The ore of this deposit is hosted within the Early Dalan Formation (modified after Liaghat et al., 2000).

(Ghavidel, 1973; Liaghat et al., 2000). These strata are overlain by about 85 m of Devonian and Early Permian Faraghan sediments composed mainly of purple and dark-gray shale with sandstone intercalations (Fig. 10). The Faraghan Formation is overlain in turn by about 120 m of Upper Permian Dalan Formation consisting of laminated limestone, dolostone, carbonaceous brown-red sandstone and, in some cases, gypsum and marl. The Dalan Formation is divided into two parts, the Early and Upper Dalan, by thin gypsum layers of the Nar Member. The Early Dalan Formation hosts the Kuh-e-Surmeh deposit (Fig. 10). The non-mineralized Upper Dalan is overlain by thin layers of shale, carbonate and anhydrite of the Triassic Kangan Formation (Solymani, 1996). The overlying Triassic Dashtak sediments are composed mainly of evaporitic dolomite and anhydrite (or gypsum) measuring about 850 m in thickness at the Kuh-e-Surmeh deposit (Fig. 10). The Jurassic sediments consist predominantly of shale, gypsum, dolostone and limestone of the Neyriz and Surmeh formations (Liaghat et al., 2000).

The orebearing Permian carbonate sequence is folded and the mineralization occurs on both flanks of an anticline. The main sulfide ore minerals are sphalerite, galena, and pyrite, while the main non-sulfide ore minerals are hydrozincite, smithsonite, and hemimorphite. Supergene weathering of the sulfide ore could have taken place at several intervals between the Paleozoic and the present day (Liaghat et al., 2000). Gossans representing the oxidation products of Zn, Fe and Pb sulfides exploited in the Kuh-e-Surmeh mineralized district, occurred not only on top of the primary ores, but they also represent the infill of deeper karstic cavities in Paleozoic carbonates. Non-sulfide minerals from Kuh-e-Surmeh have been investigated previously by several authors (Reichert and Borg, 2008). The shape of the non-sulfide orebodies ranged from bulk replacement bodies of entire blocks of the host carbonates and/or sulfides, to concretionary infilling of isolated druses and cavities with idiomorphic smithsonite and hemimorphite crystals at different levels in the upper part of the oxidation zone. Hydrozincite is also present, as well as remnants of primary sulfides. Calcite was commonly observed, either as a gangue mineral that precipitated with the primary sulfides, and as a newly formed phase associated with smithsonite.

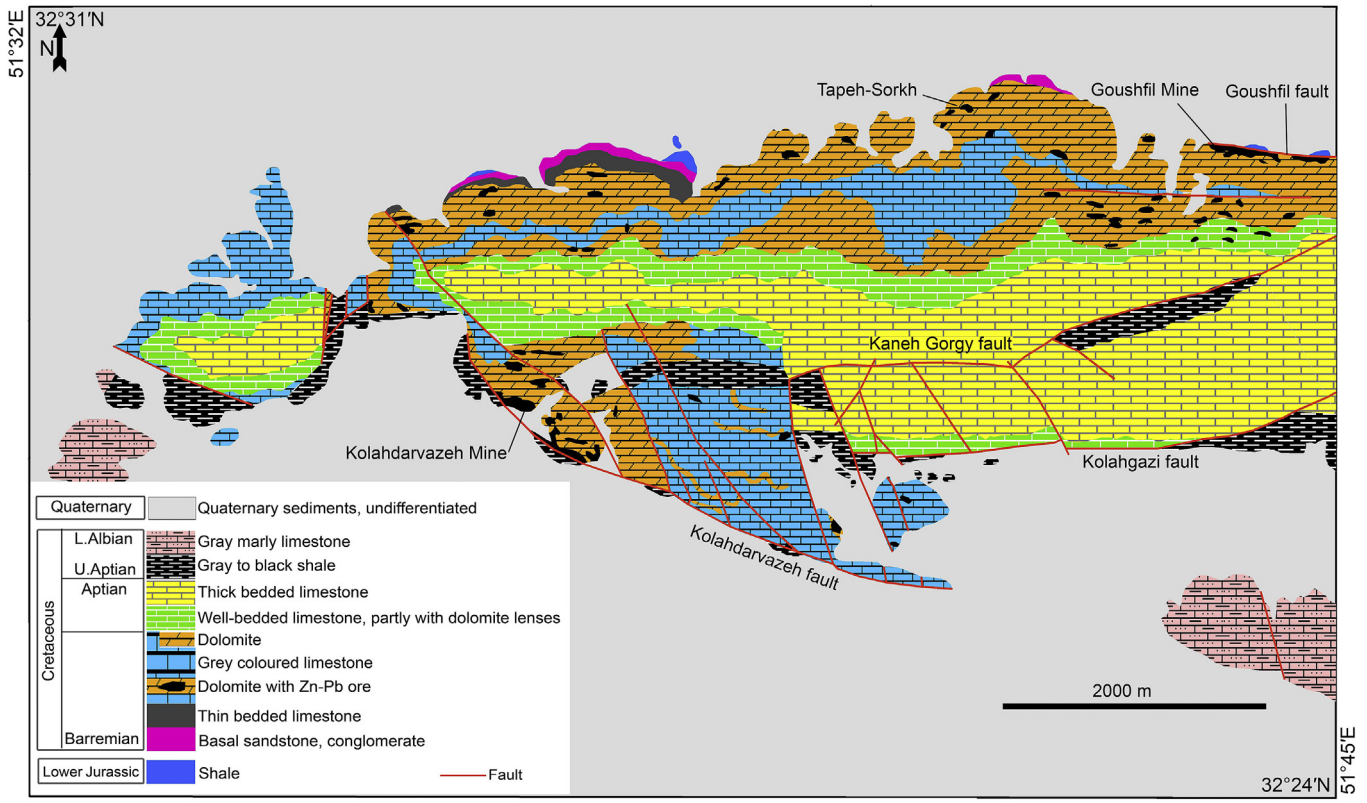

Figure 11. Schematic geological map of the Irankouh mining district (modified from unpubl. geological map, BAMA Mining Corp).

4.2. Nonsulfide Zn–Pb deposits in Iran within Mesozoic host rocks

Cretaceous carbonates are the most common host rocks of Iranian non-sulfide Zn–Pb deposits, which are largely concentrated in (1) the MEMB (Momenzadeh, 1976) in the SSZ, and (2) the YAMB in the Yazd block of the CIGS (Fig. 1 and Table 1). Approximately 66% of the Zn–Pb deposits of Iran occur in these two belts (metallogenic provinces) and include world-class examples such as Mehdiabad (in the YAMB) and Irankouh (in the MEMB) (Fig. 1).

4.2.1. Irankouh deposit

The Irankouh district comprises several Zn–Pb deposits (Figs. 11 and 12). They are located in the Irankouh Mountain Range, 20 km south of Esfahan in West-Central Iran. The Irankouh district comprises several Zn–Pb deposits, including the Goushfil pit (Borg, 2009), the Kolahdarvazeh pit, and the small Tapeh-Sorkh pit (Figs. 11 and 12). The main difference between the Goushfil and the Kolahdarvazeh pits is the nature of the ore. The Goushfil pit is characterized by large amounts of sulfide ore and a minor non-sulfide zinc ore zone. The Kolahdarvazeh mine is an open pit mine, which produces a concentrate of non-sulfide zinc ore and only shows a small amount of sulfide minerals (Fig. 13). Estimated ore reserves are more than 20 million metric tons, grading 7.4 wt.% of Zn and 2.4 wt.% of Pb. The Zn/(Zn + Pb) ratio in the Irankouh district is usually high, averaging about 0.76 (Reichert, 2007; Borg, 2009).

Zn–Pb–Ba mineralizations in the Irankouh (and in the Isfahan) district were first reported by Zahedi (1976), who, described mineralized veins occurring along faulted and fractured zones in the lower part of the hydrothermally dolomitized Barremian-Aptian limestone. Rastad (1981) suggested a diagenetic origin for such stratabound Zn–Pb–Ba–(Cu) mineralization. A very comprehensive isotopic (O, C, S and Sr isotopes) study by Ghazban et al. (1994) concluded that the deposit was an epigenetic Zn–Pb–Ba MVT-type. Hosseini-Dinani and Aftabi (2015) also proposed an epigenetic stratabound Zn–Pb–Ba mineralization related to MVT on the basis of the low Cu and Fe contents and geochemical features. Boviri and Rastad (2016) and Boveiri et al. (2017) proposed a SEDEX type mineralization for the Gushfil and Tapeh-Sorkh parts in the Irankuh district.

The regional stratigraphic sequence of the Irankouh area (Fig. 12) starts with Early Jurassic shale at the bottom, followed by Barremian–Aptian sandstone and limestone, Upper Aptian shale, and, on the top of this sequence, Tertiary sediments. Two major stratigraphic gaps can be found within this stratigraphic sequence (Fig. 12). The first one separates the Lower Jurassic shale from the Early Cretaceous strata. The second gap is located between the Cretaceous strata and the Oligocene strata (Rastad, 1981) (Fig. 12). The Early Cretaceous sediments unconformably overlie the Jurassic shales to form a continuous sequence beginning from the Barremian up to the Upper Aptian sediments (Fig. 12). The total thickness of this sequence is approximately 800 m. These Cretaceous strata comprise mainly dolomite, limestone, and minor amounts of volcanic rocks, shale and marble (Fig. 12). The Barremian and Lower Aptian sedimentary rocks host the sulfide and non-sulfide mineralization, which forms two discrete ore-bearing horizons, namely the Goushfil-Kolahdarvazeh horizon and the Goushfil-Gowdezendane horizon (Rastad, 1981; Boveiri et al., 2015) (Fig. 12).

At the Kolahdarvazeh mine, both sulfide and non-sulfide ore zones are found within the Cretaceous dolomite and limestone (Fig. 13). Sulfide mineralization occurs in several places at the contact (or close to) with shale. In most cases, the sulfide ore is partly oxidized and only local relics of sulfide minerals (mainly galena) are found. The primary sulfide mineralization consists of

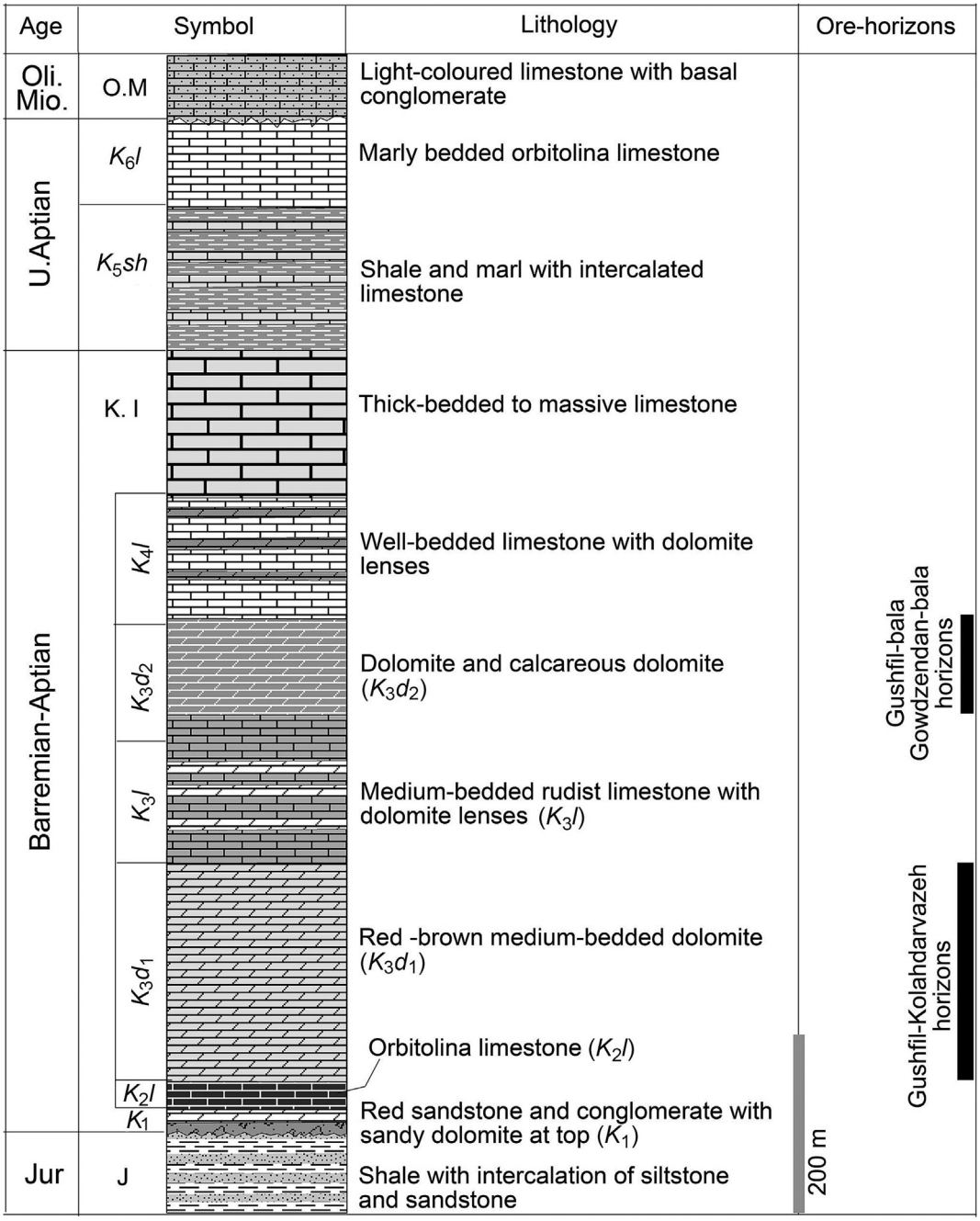

Figure 12. Regional stratigraphic sequence of the Irankouh deposit. The ore deposits are hosted within the Early Cretaceous Formations (modified after Rastad, 1981).

sphalerite, galena, with minor amounts of pyrite, and traces of marcasite, and chalcopyrite (Reichert, 2007). Associated minerals are barite and calcite mainly as veins and fracture fillings. A partial oxidation is frequently observed. In an advanced state of weathering most of the sulfide minerals have been removed and only galena is present.

Gossans representing the oxidation part of the Zn, Fe and Pb sulfide ore zones exploited in the Kolahdarvazeh mineralized districts (Fig. 13), occurred not only on the top of the primary ores, but they also represent infilling within deep karstic cavities in the Cretaceous carbonates (Reichert, 2007). Oxidation of sulfide minerals generally extends from the surface to an average of 40 to 70 m in depth. However, in several parts, Zn carbonates as well as druses filled by cerussite were also irregularly enclosed in the primary sulfide bodies down to 130 m in depth. Pb and Fe secondary minerals (cerussite, anglesite, goethite, etc.) were always associated to the Zn ores. The mineralization is considered to be the result of in situ oxidation of the primary sulfide ores by meteoric fluids, with increased acidity owing to the dissolution of substantial amounts of pyrite, which circulated through the carbonates (Reichert, 2007) (Fig. 13). The dissolution was followed by the partial to total replacement by secondary minerals of the sulfide minerals. A distinct oscillatory zoning (zinc-enriched and zinc-poor bands) in the Kolahdarvazeh deposit is considered to have been caused by variations of the water table, cyclically altering the regular deepening grade of the oxidation profiles (Reichert, 2007). Subsequent

Figure 13. (A) Overview of the Kolahdarvazeh mine. The non-sulfide zinc ore occurs in the Early Cretaceous carbonate rocks. (B) Sphalerite, galena, and pyrite can be found within shales and adjacent to the non-sulfide zinc ore hosted by carbonate rocks. (C) View of the cavities and of the fault-breccias, originally filled by the non-sulfide ore.

remobilization and redeposition within dissolution vugs and karst cavities of the newly formed oxidation minerals locally followed the early replacement process (Fig. 13B and C). Carbon and oxygen isotope measurements were applied to hydrozincite of the Kolahdarvazeh mine (Reichert, 2007). The hydrozincite samples show a range of $\delta^{18}O$ (SMOW) values between 21.9‰ and 22.9‰. The $\delta^{13}C$ values range between −3.8‰ and −7.1‰ (Reichert, 2007).

4.2.2. The Mehdiabad non-sulfide Zn–Pb deposit

The Mehdiabad deposit is situated in the Yazd Province, the central part of Iran approximately 550 km southeast of Tehran (Fig. 1). Several occurrences, namely the Calamine mine (CM), Black-Hill Ore (BHO), East Ridge (ER) and Central Valley Ore body (CVOB), have been explored and CM has been mined in historical times (Maghfouri et al., 2015; Maghfouri, 2017). Exploration during the last two decades revealed huge economic reserves, with an oxide reserve of 45.2 Mt at 7.15% Zn and 2.47% Pb and a sulfide reserve of 116.5 Mt at 7.3% Zn and 2.3% Pb. The total geological resource of this deposit includes 218 Mt at 7.20% Zn, 2.30% Pb, and 51 g/t Ag (BRGM, 1994; Reichert, 2007). In spite of its size and importance, modern data on the Mehdiabad deposit are scarce. Ghasemi (2006) investigated the geology and mineralogy of the deposit, and Reichert (2007) provided some geochemical data of the oxide ores and weathering conditions. Maghfouri (2017) also proposed a syn-sedimentary Zn–Pb–Ba–(Cu) mineralization related to SEDEX for the Mehdiabad deposit on the basis of the clastic-carbonate dominate host rocks, relation between ore minerals and rock forming minerals, structures and textures, different ore facies and geological and geochemical features.

In the Mehdiabad deposit, a thick Early Cretaceous sedimentary sequence (ECSS) is exposed, unconformable lying on top of the Jurassic Shir-Kuh granite (Fig. 14). In the following, the Early Cretaceous formations of the Yazd area (Nabavi, 1972a,b; Majidifard, 1996; Maghfouri, 2017) will be briefly described from base to top.

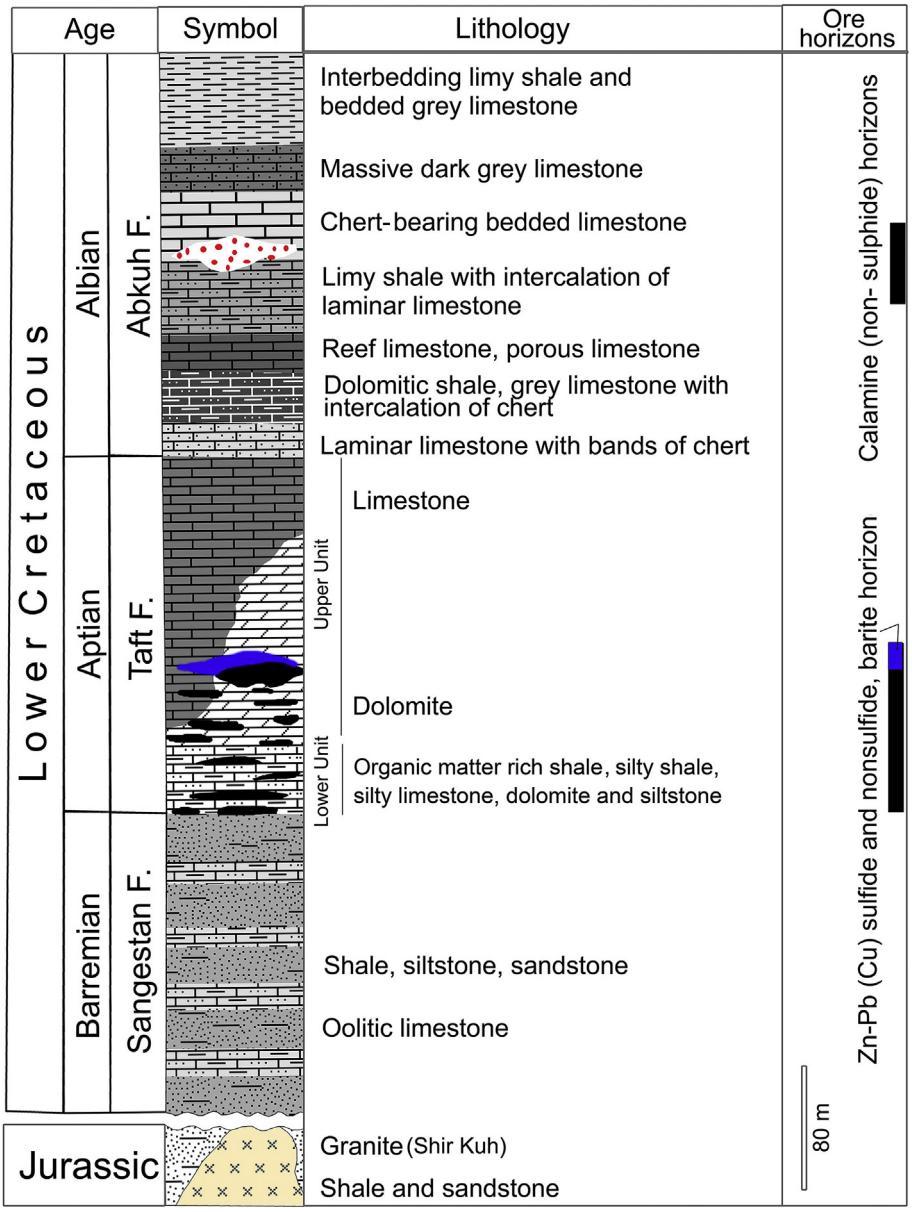

Figure 14. Regional stratigraphic sequence of the Mehdiabad deposit. The ore deposit is hosted within the Taft and Abkuh formations.

Early Cretaceous terrestrial sediments of the Sangestan Formation cover the metasediments of the Shemshak Group and the Shir-Kuh granite that initially formed a major palaeo-relief (Fig. 14). The lower part of this Formation is exclusively siliciclastic (reddish conglomerate, sandstone and siltstone) reflecting semi-arid terrestrial conditions. Toward the top of sequence, the marine influence increases and is indicated by evaporites and carbonates, locally containing calcareous algae and agglutinating foraminifera. Although the carbonates from the upper part of the Sangestan Formation have been assigned to Hauterivian (Bucur et al., 2003), the Sangestan Formation is generally considered to be of Barremian age. The Sangestan Formation is conformably overlain by thick-bedded carbonates of the (Barremian–?) Aptian Taft Formation (Fig. 13), consisting of thick-bedded to massive rudist-, algae- and orbitolinid-bearing shallow-water limestone, organic matter rich shale, silty shale, silty limestone and siltstone (Fig. 14) (e.g., Bucur et al., 2012; Schlagintweit et al., 2013a,b). The Taft Formation may reach up to 400 m in thickness (section at west BHO; Fig. 15) and is part of a large-scale carbonate platform system that characterized the Yazd Block during the Early Cretaceous (Wilmsen et al., 2013). The Zn–Pb–Ba mineralization of the Mehdiabad deposit occurs within the Taft Formation (Fig. 14) (Maghfouri et al., 2015; Maghfouri, 2017). The upper part of the Taft Formation is covered by characteristic cherty limestone of the Abkuh Formation. Above the cherty limestone, dolomitic shale with calcarenite and chert-bearing limestone, are generally identical to those seen in the drill holes. 1–10 meters-sized lenses and olistoliths of para-reef limestone become frequent in the upper part of the unit. The upper part of this unit (60–80 m) consists of limy shale and laminar limestone. The CM orebody is located in the upper part of the Abkuh Formation (Fig. 14).

Zn–Pb–Ba (Cu) mineralization of the Mehdiabad deposit occurs along two horizons that extend over a length of >4 km (Fig. 13). The sulfide and non-sulfide ores of the ore horizon I (OHI) are hosted by organic matter-rich shale, silty limestone, dolomite and silty shale

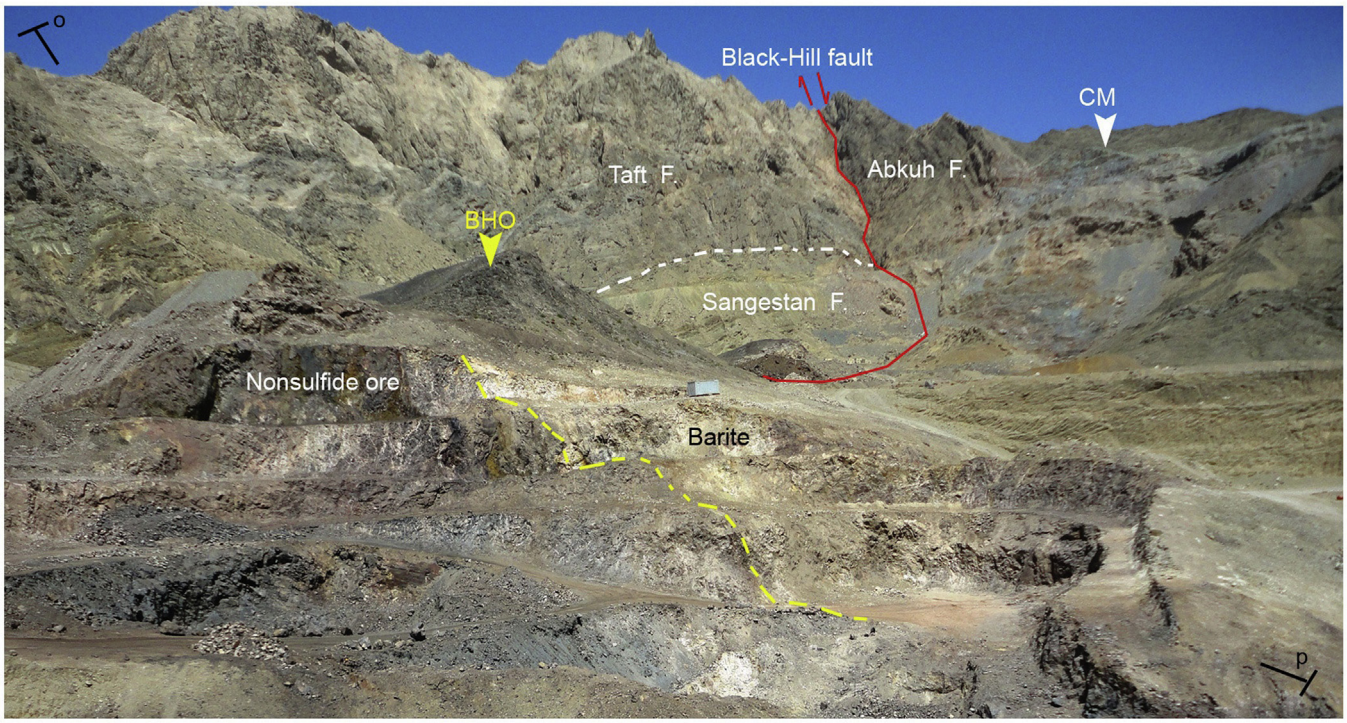

Figure 15. View of the two ore horizons forming the Mehdiabad deposit, the BHO (in the ore horizon 1) is located within the Taft Formation, while the ore horizon 2 corresponding to the CM orebody occurs within the Abkuh Formation. Mineralization in the Mehdiabad deposit locates to the East of Black-Hill fault (Location of o-p section is shown in Fig. 19D). BHO: Black-Hill Ore; CM: Calamine Mine.

of the Taft Formation, whereas non-sulfide ores of the ore horizon II (OHII) are enclosed by limy shale and thin-bedded limestone of the Abkuh Formation (Figs. 14–17) (Maghfouri et al., 2015; Maghfouri, 2017). The OHI is composed of several ore bodies, namely Black Hill Ore (BHO), Central Valley Ore Body (CVOB) and East Ridge (ER), located in a depression surrounded by hills and mountains (Figs. 15, 16 and 19D). The calamine mine (CM) exposes the OH II, which represents the highest part of the oxide ore mineralization (Figs. 17 and 19F). At sites of BHO, ER and CM, OHI is completely oxidized (Figs. 15–17), whereas the CVOB display a large proportion of sulfide minerals (Fig. 19E).

Detailed geological mapping of host rocks and structures in the Mehdiabad deposit shows that Zn–Pb–Ba–(Cu) mineralization (OHI and OHII) occurs to the east of the Black Hill Fault, a major and well-exposed fault within the Early Cretaceous sequence (Figs. 15 and 19D).

BHO veins and brecciated mineralization occurs adjacent to the Black-Hill fault (Fig. 19D). The BHO also referred as the BHO gossan consists of irregular veins of barite, quartz, chalcopyrite, pyrite, sphalerite, galena, limonite, hematite, Zn–Pb carbonate and dolomite (Fig. 15). To the east, the BHO passes into CVOB (Fig. 19D). The organic matter-rich shale, dolomite and silty limestone of the Taft Formation, host the main part of the preserved sulfide ore of the CVOB (Fig. 19E), whereas ores are enclosed is shale and siltstone in the easternmost areas. The most abundant minerals are galena, sphalerite, barite and pyrite with traces of chalcopyrite (Maghfouri, 2017).

Further to the east, the ER orebody consists of an essentially strata-bound non-sulfide mineralization developed within the silty limestone of the Taft Formation, close to the uppermost part of the Sangestan Formation, which exposes sandstone and oolitic limestone (Figs. 16A and 19D). Mineralization consists of iron (hydr-) oxide (hematite, limonite), Mn oxide and Zn and Pb carbonates (Fig. 18). A deep preserved sulfide mineralization, including galena, sphalerite and pyrite was recognized by drill cores at 100 m (Reichert, 2007; Maghfouri, 2017).

The CM represents the highest part of the exposed mineralization at Mehdiabad (Fig. 17). The mineralization is predominantly hosted within limy shale with intercalated laminar limestone of the Abkuh Formation and particularly at the contact between limy shale and chert-bearing bedded limestone (Figs. 17 and 19 F). Zn–Pb mineralization exclusively consists of non-sulfide minerals, such as smithsonite, hemimorphite, and hydrozincite (Fig. 18).

The non-sulfide zinc minerals in the Mehdiabad deposit belong to the carbonate-hosted “non-sulfide” category (Large, 2001), in which hemimorphite, hydrozincite, and smithsonite are the principal zinc-bearing minerals. Cerussite and anglesite also occur, generally associated with lenses of residual or supergene galena. A complex association of iron and manganese oxi-hydroxides (goethite, lepidocrocite, hematite), and residual clay minerals hosts the non-sulfide ore. The mineralogy of the ores is generally complex and, besides the most common Zn and Pb carbonates and silicates, it also comprises exotic species (Billows, 1941; Moore, 1972; Stara et al., 1996). The non-sulfide zinc ore of the Mehdiabad deposit can be subdivided into a red zinc ore (RZO) and a white zinc ore (WZO) (Fig. 18). The RZO is rich in Zn (up to 30%), iron (17%) and other metals such as Pb and As (Reichert, 2007). In contrast, the WZO typically shows high zinc grades (up to 40%) and low concentrations of iron (<7%) with minor Pb and As (Reichert, 2007). The RZO is dominant in the OHI, while the WZO is characteristic of the OHII. Common minerals of the RZO are Fe-oxyhydroxides, goethite, hematite, hemimorphite, hydrozincite, smithsonite, and cerussite. Hemimorphite is one of the most important zinc minerals of this ore-type. Most common minerals of the WZO are hydrozincite, smithsonite, and hemimorphite. Iron-bearing minerals are rare compared with the RZO. Hemimorphite is less common compared to what observed in the RZO.

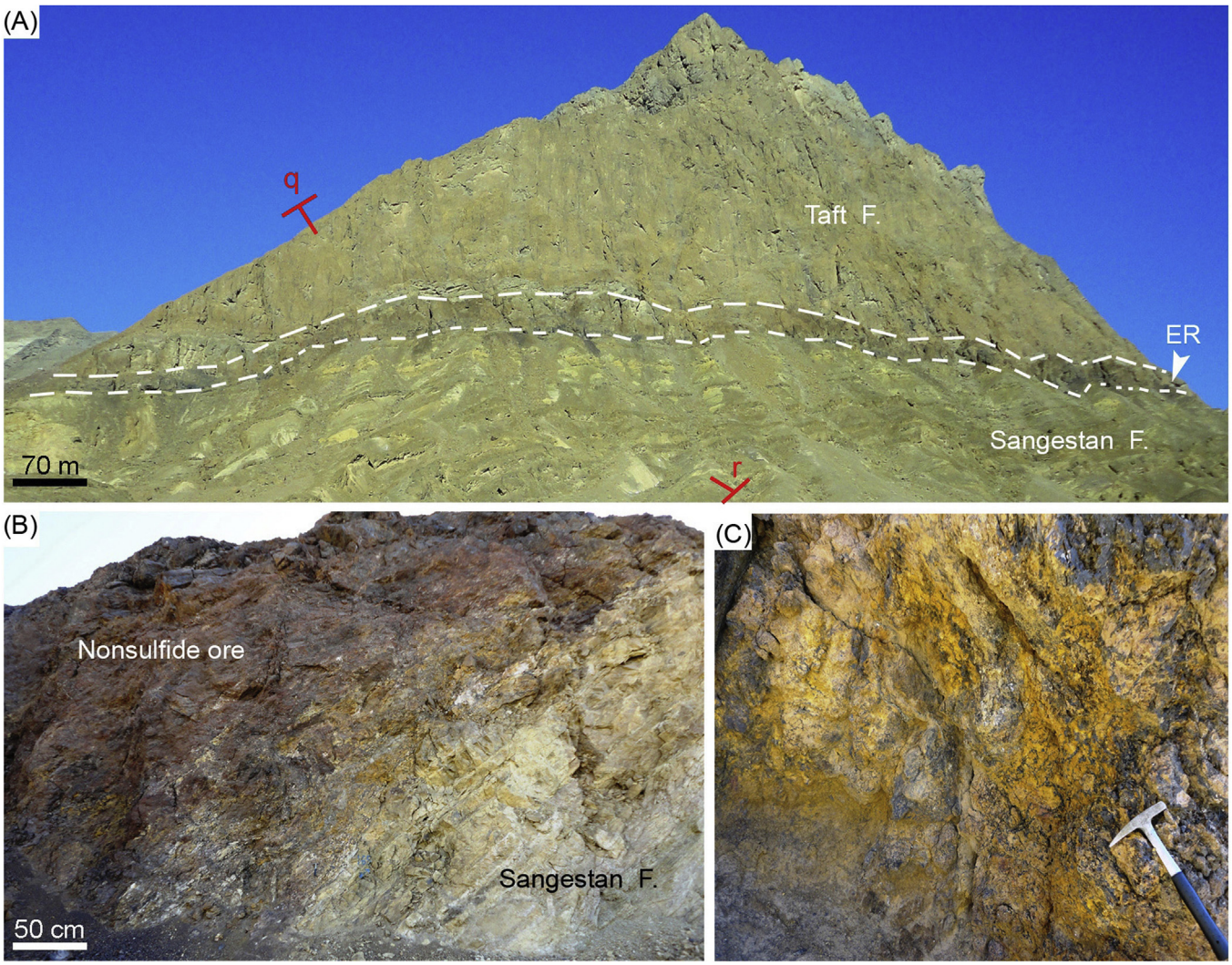

Figure 16. (A) View of the ER nonsulfide mineralization between the Sangestan and Taft Formations (Location of q–r section is shown Fig. 19D). (B) Non-sulfide ore of the OH I covering the Sangestan. (C) Aspect of the Zn-nonsulfide ore in the gossan.

Carbon and oxygen isotope measurements have been made in ore samples of the Mehdiabad deposit (Reichert, 2007). The hydrozincite samples show a restricted range of $\delta^{18}O$ values between 20.4‰ and 21.9‰. The $\delta^{13}C$ values are more variable and range between −0.4‰ and −3.8‰ (Reichert, 2007). This signature is similar to that of smithsonite samples, which have been analyzed by Boni et al. (2003) and Gilg and Boni (2004). It indicates that at least two isotopically different sources of carbon contributed to the formation of zinc carbonates. The roughly constant $\delta^{18}O$ values and the variably low- to medium-depleted $\delta^{13}C$ values reflect the influence of meteoric water associated with subaerial exposure (Allen and Matthews, 1982; Lohmann, 1988) and point to the precipitation of the zinc carbonates within the vadose and/or phreatic zone (Allen and Matthews, 1982; Reichert, 2007; Borg, 2015). The isotopically light component of the carbon is probably the result of dissolved CO_2 derived from the decay of organic matter (Criss, 1995).

5. Discussion

5.1. Critical parameters on the formation of non-sulfide deposit

Based on studies of Borg (2005), Reichert (2007) and Reichert and Borg (2008), non-sulfide zinc ores in Iran are mostly secondary and was formed by the supergene oxidation of primary sulfide deposits (Figs. 19 and 20A), although there is some evidence for primary origin of non-sulfide zinc minerals in Irankouh (Reichert, 2007). Silicate-dominated non-sulfide Zn deposits, such as those in the Upper Proterozoic volcano-sedimentary successions in the Americas and Australia (e.g., Vazante, Brazil; Beltana, Australia), have not been identified in Iran. Non-sulfide zinc deposits in Iran are essentially zinc-rich gossans exposing the replacement of sphalerite by smithsonite, hemimorphite and hydrozincite. In addition, zinc sulfide deposits originally contained galena, copper and lead sulfides. As these minerals are oxidized, they may be replaced by copper and lead carbonates, oxides, and even secondary sulfides like chalcocite.

Direct-replacement non-sulfide deposits in Iran represent the supergene evolution of carbonate hosted-type (MVT-type), carbonate replacement-type and Sedex deposits (Fig. 20A). Deposits characterized by carbonate environment (Fig. 19A and C–F), such as Mehdiabad, Irankouh, Kuh-e-Surmeh and Angouran tend to be mineralogically simple and are dominated by smithsonite, hemimorphite, and hydrozincite. In addition, like at Mehdiabad and Irankouh deposits Zn-rich Mn minerals, copper-zinc carbonates and complex arsenic minerals are also present. The occurrence of primary iron sulfide minerals tends to produce sufficient acid

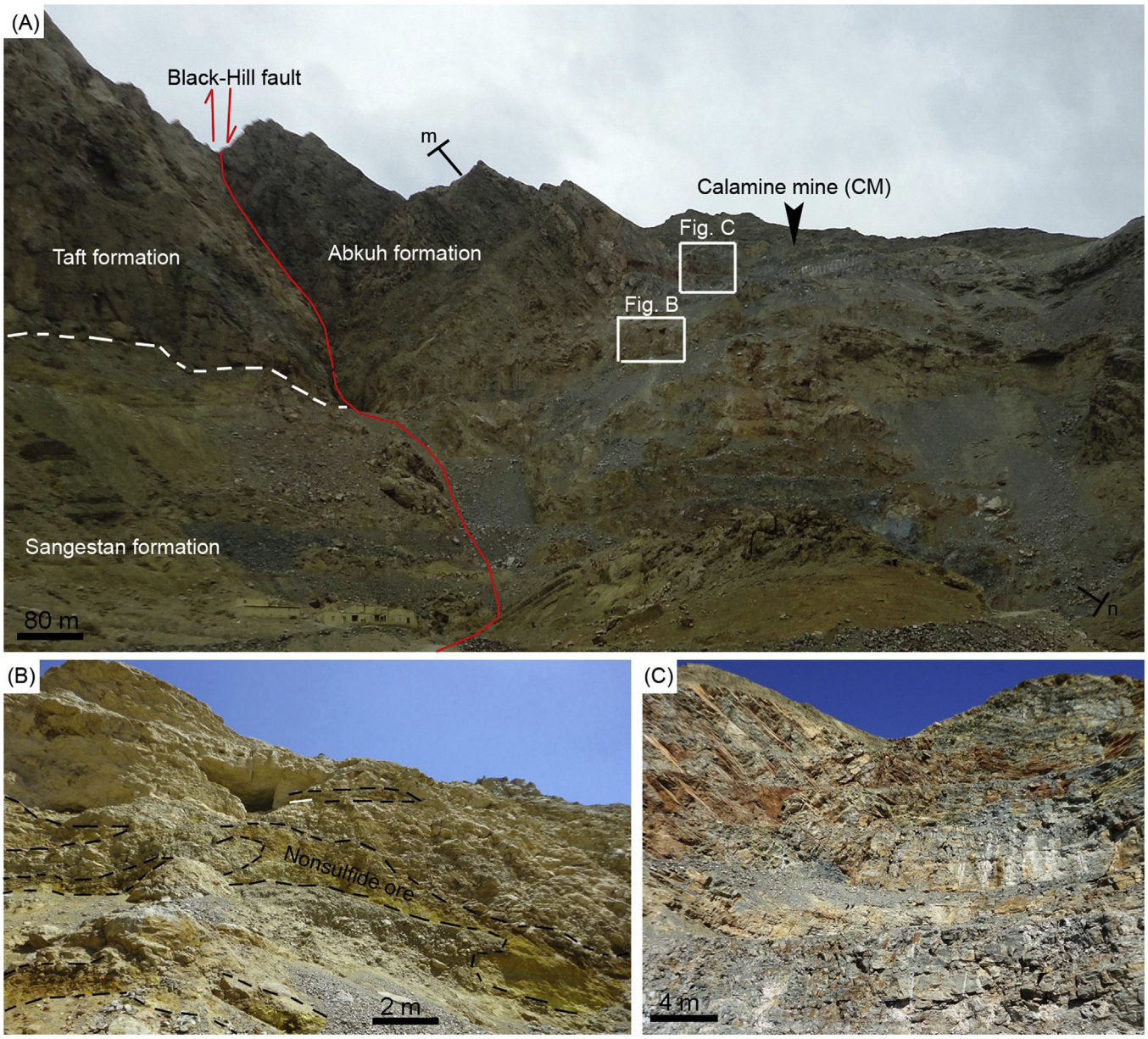

Figure 17. (A) View of the CM mineralization hosted by the Abkuh Formation to the east of Black-Hill fault (Location of m–n section is shown in Fig. 19F). (B) Detailed view of the CM non-sulfide mineralization in the chert-bearing limestone of the Abkuh Formation. (C) Detailed view of the non-sulfide mineralization within shale and laminar limestone.

during weathering to completely leach zinc from the near-surface environment (Figs. 7, 9 and 16). For example, the OHI in Mehdiabad deposit is oxidized up to a depth of 100 m (Figs. 15 and 19D); despite high primary grade in the sulfide zone (approx. 12% zinc and 5% lead), the gossan cap and oxidized zone show complete non-sulfide minerals features (Fig. 15). The sulfide mineral content in this horizon is dominated by pyrite, which constitutes more than 30 vol.% of the ore. The H_2SO_4 generated by pyrite oxidation, together with Fe^{3+} as an oxidant (Reichert, 2007), allows for the complete removal of zinc, which is highly mobile in low pH conditions (Andrew-Jones, 1968). Such complete leaching results in the formation of a gossan with iron oxides, cerussite, hemimorphite, and copper carbonates in the BHO and ER.

Like supergene copper "oxide" deposits (Chávez, 2000), non-sulfide zinc deposits in Iran formed by oxidation of a sulfide-bearing protolith (Fig. 20A) following a series of reactions between meteoric waters, metal sulfides, and reactive host rocks (Borg, 2005, 2015; Reichert and Borg, 2008; Choulet et al., 2013). Dissolution of sulfides by O_2 and Fe^{3+} provides low pH, sulfate-bearing solutions, which are able to transport metals. Although sphalerite and, to a much lesser extent, galena are very susceptible to oxidation (Bladh, 1982; Boyle, 1994), they produce relatively small quantities of acid sulfate-bearing solutions compare to iron sulfides (Williams, 1990). Sphalerite is also extremely susceptible to oxidation by moderately thermophilic (30–50 °C) bacteria in a highly oxidized, acidic, ferric sulfate-rich environment. It is normally consumed by oxidation before pyrrhotite, pyrite, galena, or chalcopyrite (Rose et al., 1979). Normally, acids produced by such oxidation of sulfide minerals would be expected to effectively remove zinc from the system (Sangameshwar and Barnes, 1983). However, given the buffering action of the carbonate host rocks, sulfuric acid generated by the oxidation of pyrite and other sulfide minerals will be neutralized, thereby ensuring a buffered, nearly

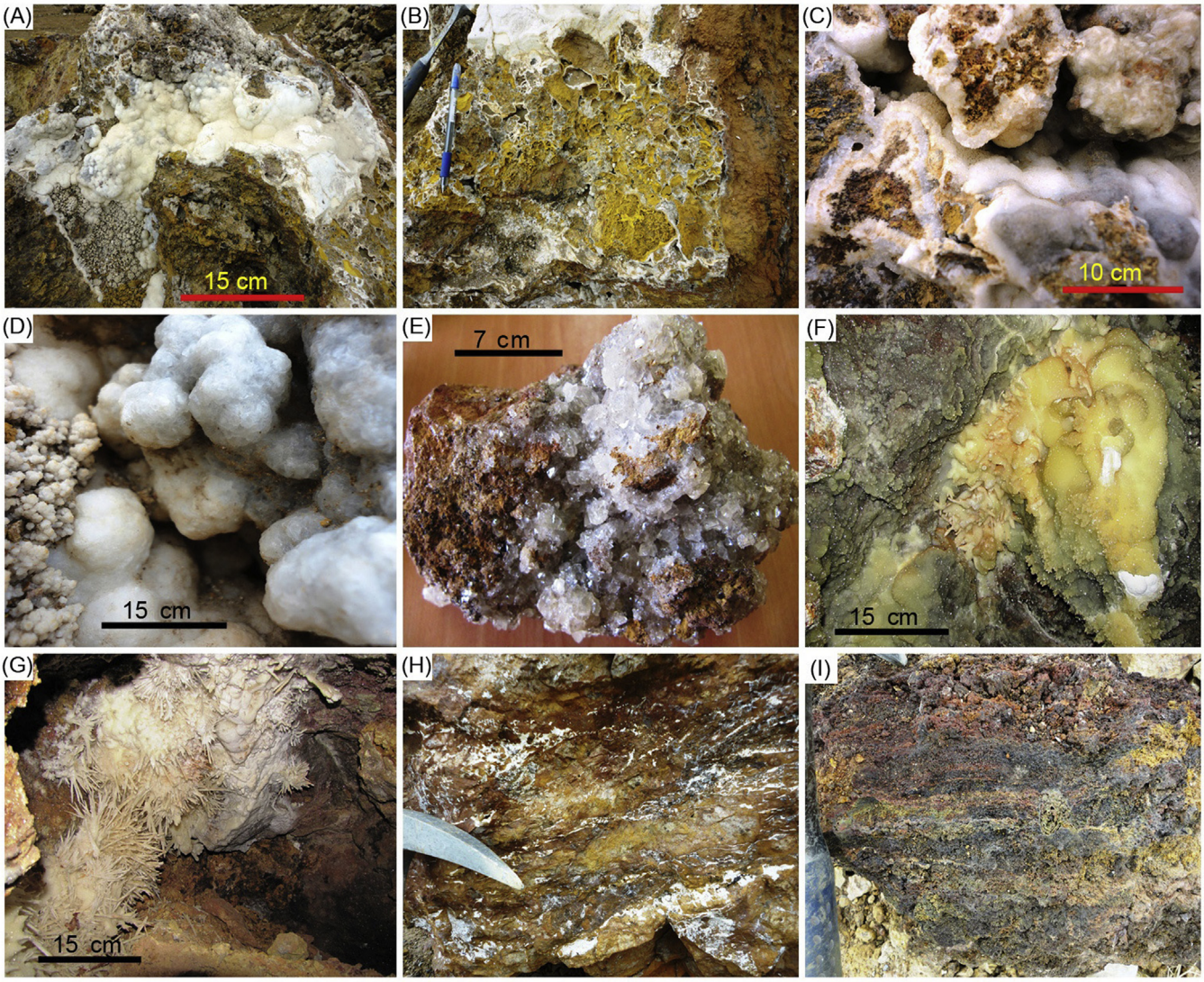

Figure 18. Images of supergene non-sulfide zinc samples from the Mehdiabad deposit. (A and B) WZO minerals coating RZO minerals. (C) Colloform smithsonite forming the WZO. (D) Botryoidal smithsonite filling vug. (E) Crystalline hemimorphite (Hem) covering hematitic and goethitic limestone. (F) Stalactitic smithsonite (Sm). (G) Radial and euhedral cerussite (Cer) growing on Fe oxide bearing limestone. (H) Limestone replaced by brown smithsonite (Sm) that is in turn replaced by white hydrozincite (hyz). (I) RZO made of smithsonite and Fe-oxides.

neutral pH environment. Under these conditions, zinc carbonate like smithsonite is the normal products of oxidation of sphalerite deposits through contact with meteoric waters (Reichert, 2007; Reichert and Borg, 2008; Choulet et al., 2013). The isotopic pattern of the hydrozincite samples of Kolahdarvazeh deposit show close ranged $\delta^{18}O$ values and a more variable range of $\delta^{13}C$ data (Reichert, 2007). The $\delta^{13}C$ values of the Kolahdarvazeh are up to 3.3‰ lower than those from hydrozincite of Mehdiabad (Reichert, 2007). The formation of the hydrozincite should be potentially influenced by an isotopically light component of carbon as a result of dissolved CO_2 derived from the decay of organic matter. However, the hydrozincite of the Kolahdarvazeh mine shows lower $\delta^{13}C$ values than its pendant from Mehdiabad deposit (Reichert, 2007). This suggests a more important role of organic and meteoric CO_2 than in Mehdiabad (Reichert, 2007). A possible reason is a variable contribution of carbonate carbon from the limestone and/or the dolomite host rock and reduced organic carbon derived from the overlying soils and is comparable to pedogenic carbonates (Cerling, 1984; Coniglio et al., 1996).

5.2. Genesis and controls on the formation of Iranian non-sulfide deposits

Some of the key controls on the formation of carbonate-hosted non-sulfide Zn–Pb deposits are the nature and availability of near-surface sulfide protore, lithology, subaerial exposure, tectonic uplift, climate and favorable hydrology (Large, 2001; Hitzman et al., 2003). In the Iranian non-sulfide deposits, tectonic uplift resulted in the near-surface exposure of the sulfide protores enabling their oxidation under a favorable climate (Fig. 20A and B) (Reichert, 2007; Reichert and Borg, 2008; Borg, 2015). Tectonic uplift and related faulting during post-sulfide mineralization deformation events played a role for the fracturing of hosting carbonates (Fig. 20B) (Aghanabati, 1998, 2004), facilitating the action of meteoric waters (Fig. 20C). Climate also strongly controlled the oxidation and therefore the transport and the redeposition of metals. The most favorable conditions for oxidation are achieved under arid (Reichert and Borg, 2008; Borg, 2015) to temperate (Hitzman et al., 2003; Santoro et al., 2013) climates,

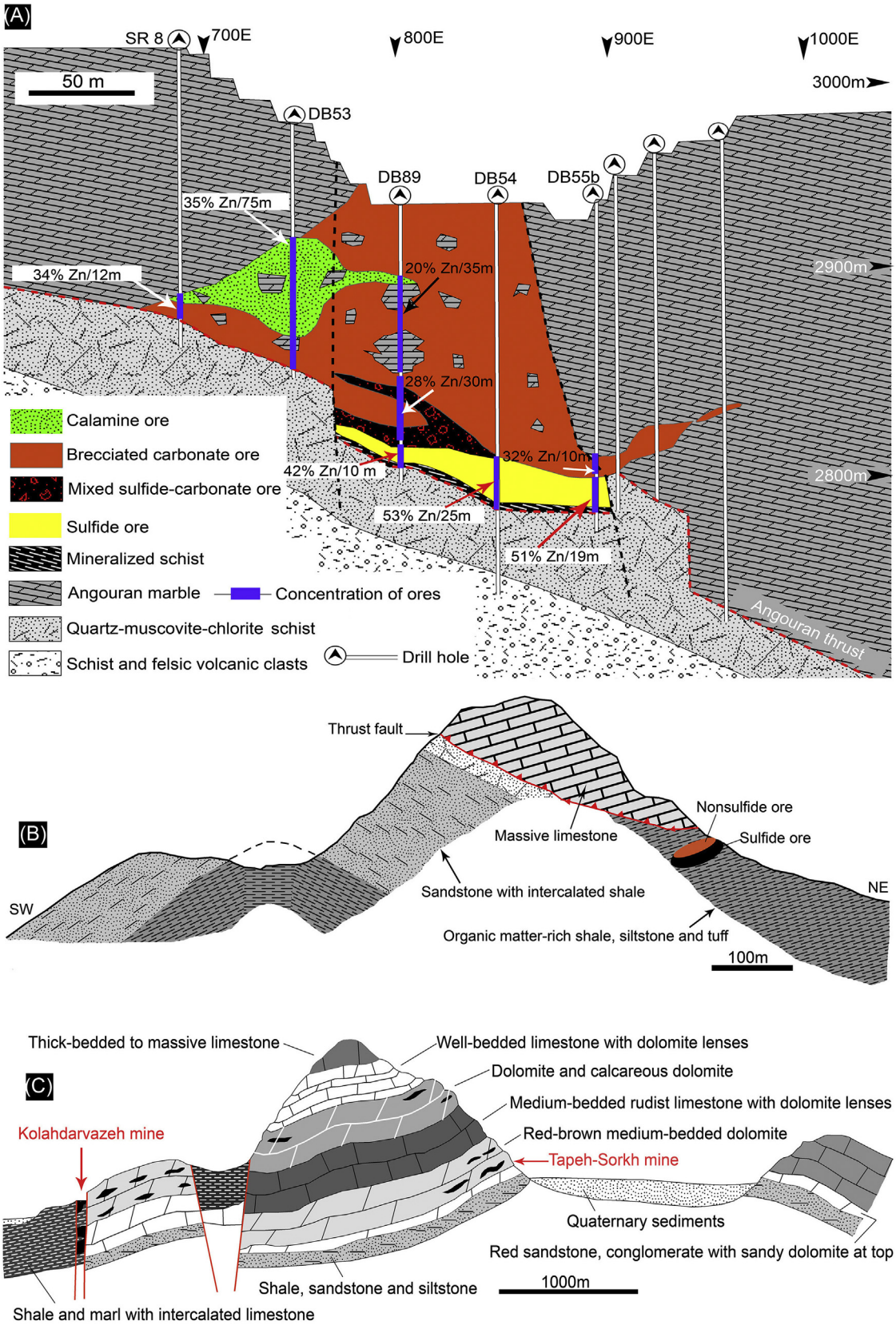

Figure 19. Cross-sections and plan view of the ore sequence and extension of non-sulfide mineralization in Iranian deposits. (A) NE–SW cross section (800 N) of the Angouran pit through the ore body; the pipe-like geometry are shown together with the distribution of the various ore types and the drill hole intervals with Zn assays (modified after Daliran et al., 2013). (B) Geological cross section of the Haft-har deposit showing the small-scale folding of the sequence. (C) General section of the Irankouh mining district, including Kolahdarvazeh mine and Tapeh-Sorkh mine (Rastad, 1981). (D) Schematic cross section of the OHI in the Mehdiabad deposit, including the o-p profile along the BHO mineralization (Fig. 15) and the q–r profile along the ER mineralization (Fig. 16A). (E) N–S cross section of the ore sequence with extension of sulfide and non-sulfide ore mineralizations in the CVOB (Mehdiabad deposit). (F) Schematic NNW–SSE section of the folded and faulted strata at the Calamine Mine area in the Mehdiabad deposit (Location of the m–n section is shown in Fig. 17A). The non-sulfide-bearing strata are repeated due to folding and thrusting (modified after Nosratian, 1991).

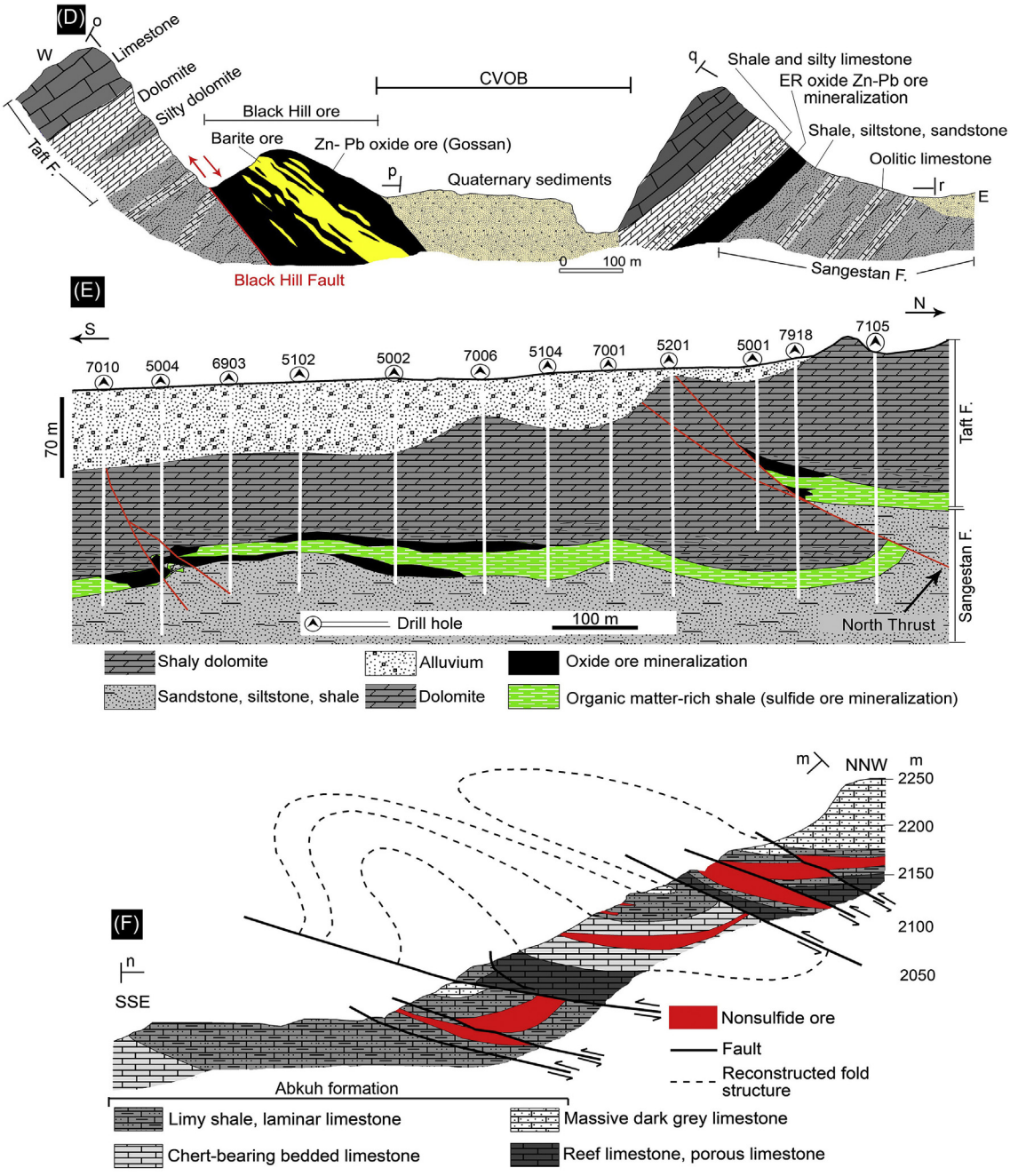

Figure 19. (*continued*).

in which a maximum amount of metals is available for transport by supergene solutions. As the biogenic activity in the soil is limited, more oxygen is available for sulfide oxidation, and consequently a lot of metals are liberated into the solutions (Reichert and Borg, 2008). It is important to note, that the climate as well as the local geology (fragmentation, karstification) of the carbonate host rocks influence the O_2 and CO_2 concentrations of the descendent fluids, and thus, the pH and the ability of the fluid to dissolve the carbonate host rock (Fig. 20C). Reichert and Borg (2008) showed that arid environments provided the best conditions for the oxygen-driven oxidation of sulfide ores. The oxidation by Fe (III) is not included here, since Fe (III) itself is provided by oxygen and affects the oxidation process only on a regional scale. In arid environments like in Iran, the dissolved O_2 reaches its maximum concentration, compared to other climates, and will not be consumed by biological activities within soils (Reichert, 2007; Reichert and Borg, 2008). The groundwater table in arid climates is commonly low. This will lead to an opening of the water-filled pores and joints after an individual rainfall event and will thus provide an inward flow of gasses (O_2, CO_2) to any available sulfide ore body (Reichert, 2007; Reichert and Borg, 2008; Choulet et al., 2013). This system will commonly change

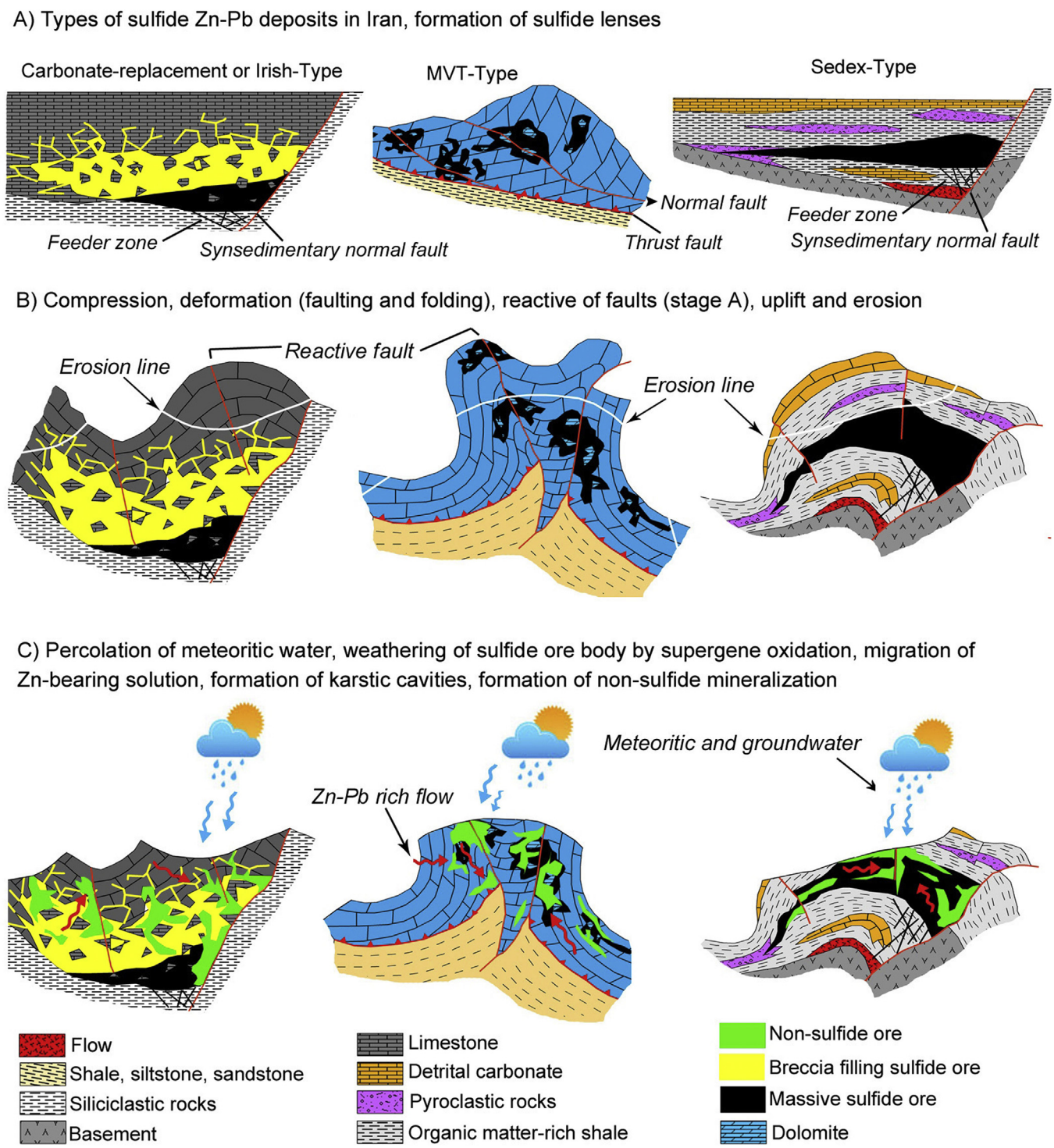

Figure 20. Development of the Iranian non-sulfide Zn–Pb deposits during the evolution of tectonic. (A) Different types of the sediment hosted Zn–Pb deposits (Sedex-type, MVT-type and Irish-type) formed in Iran. These deposits occur in carbonate and siliciclastic rocks, also the normal faults are playing a role of conduits to drive Zn–Pb rich fluids from depth to surface. (B) Since post-sulfide mineralization, the areas have recorded compressive tectonics, leading to the formation of the fold-and-thrust. Inversion tectonics affected the normal faults, which were reactivated as thrusts. (C) During stage C, regional uplift and erosion contributed to exhume the host rocks and the Zn–Pb sulfides. When the water table has fallen below the sulfides of protore, their supergene oxidation may have started; it was accompanied by the simultaneous extension of the karst network in the carbonate formations and the coeval to subsequent replacement of sulfide ores by non-sulfides ores.

to a highly permeable system due to (karstic) dissolution processes of the carbonate host rock (Fig. 20C). Due to the limited availability of water in arid and hyper-arid climates, the fluids, which have been generated during the oxidation process, would be highly enriched in zinc and other metals (Fig. 20C). These high metal concentrations support an effective precipitation of non-sulfide base metal minerals (Fig. 20C). These high element concentrations support an effective precipitation process within the carbonate host rock. Thus, an arid or semi-arid climate of Iranian non-sulfide environments provides best conditions for the

oxidation of a sulfide ore and also provides the best conditions for the preservation of a non-sulfide ore-body (Fig. 20). In arid environments of Mehdiabad, Irankouh, Kuh-e-Surmeh, Zarigan and Haft-har districts, hydrozincite is much more common than smithsonite at the surface, while carbonates are dominant with respect to hydrated phases in depth. Takahashi (1960) explained this in terms of CO_2 content, which results from the dissolution of carbonate rocks by acids released by the weathering of sulfide minerals. Above the water table, this carbon dioxide escapes to the atmosphere, thereby lowering the activity of CO_2 and stabilizing hydrozincite. Below the water table, carbon dioxide is soluble and, owing to its slow rate of diffusion, results in an elevated activity of CO_2 and, consequently to the stability of smithsonite.

6. Conclusion

The main economic minerals of the "non-sulfide" type deposits in Iran consist of Zn (hydro-) carbonates and silicates (smithsonite, hydrozincite, and hemimorphite) associated with Fe and Mn oxy (hydroxides) and residual clays. The mineralization is considered to be the result of in situ oxidation and replacement (with limited transport, locally) of the primary sulfide phases, due to meteoric fluids circulating in the carbonate rocks. Consequently, non-sulfide Zn ore deposits that originate from stratiform sulfide lenses formed either by sulfide replacement or by infilling of karst conduits due to precipitation or internal sedimentation.

Although the six studied ore deposits present a similar first-order mineralogical evolution, we have observed small discrepancies between these sites owing to various local and external factors. Climate conditions were generally similar in Mehdiabad, Irankouh, Kuh-e-Surmeh, Zarigan and Haft-har and different with Angouran, but studied zones have experienced differential deformation, as raised by their variable structural features. This has a direct influence on the amount of uplift and the local erosion of the strata. This also controls the water table level and the ability to concentrate zinc in carbonate, silicate and hydrated phases. As in most supergene deposits, moderate tectonic uplift and brittle fracturing are required, together with favorable climatic conditions, for the development of extensive weathering profiles. The age of the main weathering phase is still uncertain, but in Mehdiabad deposit indirect geological evidence suggests post-Cretaceous oxidation.

The association of carbonate-hosted non-sulfide zones with underlying massive sulfides in combination with the characteristics of the non-sulfide ore suggests that most of the known non-sulfide mineralized zones in Iran are the result of supergene, direct replacement process of CH and SEDEX deposits. Zinc and Pb non-sulfides can also be used as indirect indicator minerals for exploration of MVT, SEDEX, Irish-type, and carbonate replacement and vein-type Zn–Pb deposits.

References

Aghanabati, A., 1998. Major sedimentary and structural units of Iran (map). Geosciences 7, 29–30.

Aghanabati, A., 2004. Geology of Iran. Geological Survey of Iran, 600 p.

Aghazadeh, M., Hou, Z., Badrzadeh, Z., Zhou, L., 2015. Temporal–spatial distribution and tectonic setting of porphyry copper deposits in Iran: constraints from zircon U–Pb and molybdenite Re–Os geochronology. Ore Geology Reviews 70, 385–406.

Alavi, M., 1996. Tectonostratigraphic synthesis and structural style of the Alborz Mountains system in northern Iran. Journal of Geodynamics 11, 1–33.

Allen, J.R., Matthews, R.K., 1982. Isotope signatures associated with early meteoric diagenesis. Sedimentology 29, 297–817.

Andrew-Jones, D.A., 1968. The application of geochemical techniques to mineral exploration. Colorado School of Mines Mineral Industries Bulletin 11, 1–31.

Annels, A.A., 2005. New Ideas Concerning the Genesis of the Angouran Zn–Pb Deposit, NW Iran. European Science Foundation. Exploratory Workshop "Nonsulfide Zn–Pb Ores", 21–23 April 2005, Iglesias (Italy), Abstract Volume, 3–4.

Appold, M.S., Monteiro, V.S., 2009. Numerical modeling of hydrothermal zinc silicate and sulfide mineralization in the Vazante deposit, Brazil. Geofluids 9, 96–115.

Babakhani, A.R., Ghalamghash, J., 1990. Geological map of Iran, 1:100,000 series sheet Takht-e-Soleiman. Geological Survey of Iran, Tehran.

Billows, E., 1941. I minerali della Sardegna ed i loro giacimenti. Rendiconti Università di Cagliari, pp. 331–335.

Bladh, K.W., 1982. The formation of goethite, jarosite, and alunite during the weathering of sulfide-bearing felsic rocks. Economic Geology 77, 176–184.

Boland, M.B., Kelly, J.G., Schaffalitzky, C.S., 2003. The Shaimerden supergene zinc deposit, Kazakhstan: a preliminary examination. Economic Geology 98, 787–795.

Boni, M., Mondillo, N., 2015. The "Calamines" and the "Others": the great family of supergene nonsulfide zinc ores. Ore Geology Reviews 67, 208–233.

Boni, M., 2014. Supergene Nonsulfide Zinc Ores. State of the Art. Abstract at 21st General Meeting of the International Mineralogical Association, Sandton South Africa.

Boni, M., Gilg, H.A., Balassone, G., Schneider, J., Allen, C.R., Moore, F., 2007. Hypogene Zn carbonate ores in the Angouran deposit, NW Iran. Mineralium Deposita 42, 799–820.

Boni, M., Gilg, H.A., Aversa, G., Balassone, G., 2003. The "Calamine" of SW Sardinia (Italy): geology, mineralogy and stable isotope geochemistry of a supergene Zn-mineralization. Economic Geology 98 (4), 731–748.

Borg, G., 2015. A review of supergene nonsulphide zinc (SNSZ) deposits - the 2014 update. In: Archibald, S.M., Piercey, S.J. (Eds.), Current Perspectives of Zinc Deposits. Irish Association for Economic Geology, Dublin, pp. 123–147.

Borg, G., 2009. The influence of fault structures on the genesis of supergene zinc deposits. Society of Economic Geologists Special Publication 14, 121–132.

Borg, G., 2005. Geological and economical significance of supergene nonsulphide zinc deposits in Iran and their exploration potential. In: Geological Survey of Iran (Ed.), Mining and Sustainable Development. 20th World Mining Congress, 7–11 November 2005, Tehran, Iran, pp. 385–390.

Borg, G., Karner, K., Buxton, M., Armstrong, R., Merwe, Schalk W. v.d, 2003. Geology of the Skorpion supergene zinc deposit, southern Namibia. Economic Geology 98, 749–771.

Borg, G., Kärner, K., 2001. A preliminary appraisal of the sedimentary, volcanic, and tectonic setting of the Skorpion nonsulphide Zn deposit, southern Namibia. Geological Society of America Abstracts with Programs 33, A-337.

Boveiri, M., Rastad, E., Mohajjel, M., Nakini, A., Haghdoost, M., 2015. Structure, texture, mineralogy and genesis of sulfide ore facies in Tappehsorkh detrital-carbonate hosted Zn-Pb- (Ag) deposit, South of Esfahan. Scientific Quarterly Journal, Geosciences 25, 221–236.

Boviri, M., Rastad, E., 2016. Nature and origin of dolomitization associated with sulphide mineralization: new insights from the Tappehsorkh Zn-Pb (-Ag-Ba) deposit, Irankuh Mining District, Iran. Geological Journal. http://dx.doi.org/10.1002/gj.2875.

Boveiri, M., Rastad, E., Peter, J., 2017. A sub-seafloor hydrothermal syn-sedimentary to early diagenetic origin for the Gushfil Zn-Pb-(Ag-Ba) deposit, south Esfahan, Iran. Neues Jahrbuch für Mineralogie-Abhandlungen Journal of Mineralogy and Geochemistry 194 (1), 61–90.

Boyle, D.R., 1994. Oxidation of massive sulfide deposits in the Bathurst mining camp, New Brunswick: natural analogues for acid drainage in temperate climates. In: Alpers, C.N., Blowes, D.W. (Eds.), Environmental Geochemistry of Sulfide Oxidation, American Chemical Society Symposium Series, vol. 550, pp. 535–550.

BRGM, 1994. Mehdiabad Lead-Zinc Deposit, Prefeasibility Study. Geological Assessment Report (Unpubl. internal report).

Brugger, J., McPhail, D.C., Wallace, M., Waters, J., 2003. Formation of willemite in hydrothermal environments. Economic Geology 98, 819–835.

Brugger, J., McPhail, D.C., Waters, J., Wallace, M., Lees, T., 2001. Formation of willemite in hydrothermal environments. Geological Society of America Abstracts with Programs 33, A-33.

Bucur, I.I., Rashidi, K., Senowbari-Daryan, B., 2012. Early Cretaceous calcareous algae from central Iran (Taft Formation, south of Alibad, near Yazd). Facies 58, 605–636.

Bucur, I.I., Senowbari-Daryan, B., Majidifard, M.R., 2003. Neocomian microfossil association from the Taft area near Yazd (Central Iran). Facies 49, 217–222.

Cerling, T.E., 1984. The stable isotopic composition of modern soil carbonate and its relationship to climate. Earth and Planetary Science Letters 71, 229–240.

Chávez Jr., W.X., 2000. Supergene oxidation of copper deposits: zoning and distribution of copper oxide minerals. Society of Economic Geologists Newsletter 41 (1), 10–21.

Choulet, F., Charles, N., Barbanson, L., Branquet, Y., Sizaret, S., Ennaciri, A., Badra, L., Chen, Y., 2013. Non-sulfide zinc deposits of the Moroccan High Atlas: multi-scale characterization and origin. Ore Geology Reviews 56, 115–140.

Coniglio, M., Myrow, P., White, T., 1996. Stable oxygen and carbon isotope compositional fields for skeletal and diagenetic components in New Zealand Cenozoic nontropical carbonate sediments and limestones: a synthesis and review. New Zealand Journal of Geology and Geophysics 39, p. 93–10.

Criss, R.E., 1995. Stable isotope distribution. variations from temperature, organic and water-rock interactions. In: Ahrens, T.J. (Ed.), Global Earth Physics: A Handbook of Physical Constants. American Geophysical Union, Washington, D.C., pp. 292–307

Daliran, F., Pride, K., Walther, J., Berner, Z.A., Bakker, R.J., 2013. The Angouran Zn (Pb) deposit, NW Iran: evidence for a two stage, hypogene zinc sulfide–zinc carbonates mineralization. Ore Geology Reviews 53, 373–402.

Daliran, F., Borg, G., Armstrong, R., Vennemann, T., Walther, J., Woodhead, J.D., 2009. Nonsulphide Zinc Deposits, Iran. The Hypogene Emplacement and Supergene Modification History of the Angouran Zinc Deposit, NW-Iran. Berichte zur Lagerstätten- und Rohstoffforschung, vol. 57. BGR, Hannover, 75 pp.

Daliran, F., Borg, G., 2004. Nonsulphide Zinc Deposits, Iran: a Preliminary Study of the Zinc Ores at Angouran Mine, NW-Iran. BGR Reihe Berichte zur Lagerstätten- und Rohstoffforschung. BGR, Hannover, 103 pp.

Daliran, F., 2003. Geology, Mineralogy, and Models of Hypogene and Supergene Metallogeny of the Angouran Mixed Sulphide–nonsulphide Zinc Deposit, NW—Iran. Proceeding of Nonsulphide Zinc Workshop, Anglo American, Jo'Burg, 17–19.09.2003 (4 pp).

Gazanfari, F., 1991. Metamorphic and Igneous Petrogenesis in NE of Takab with Special Regard to Zinc Mineralization in the Angouran Mine (Unpublished MSc Thesis). Teheran University, 530 pp. (in Farsi).

Ghazban, F., McNutt, R.H., Schwarcz, H.P., 1994. Genesis of sediment-hosted Zn-Pb-Ba deposits in the Iran Kouh district, Esfaha area, west-Central Iran. Economic Geology 89, 1262–1278.

Ghasemi, M., 2006. Formation Mechanism of the Mehdi Abad Zn–Pb Deposit and its Comparison with Other Near Lead and Zinc Deposits (Unpublished M.Sc. Thesis). Research Institute of Earth Sciences, Geological Survey of Iran, 238 p.

Ghorbani, M., 1999. Petrological Study of Cenozoic–Quaternary Magmatic Rocks and Metallogeny of Takab Area (Unpublished PhD Thesis). Shahid Beheshti University of Tehran, 430 pp. (in Farsi).

Gilg, H.A., Boni, M., Balassone, G., Allen, C.R., Banks, D., Moore, F., 2006. Marble-hosted sulphide ores in the Angouran Zn–(Pb–Ag) deposit, NW Iran: interaction of sedimentary brines with a metamorphic core complex. Mineralium Deposita 41, 1–16.

Gilg, H.A., Boni, M., 2004. Stable isotope studies on Zn and Pb carbonates: could they play a role in mineral exploration?. In: Pecchio, M., Andrade, F.R.D., D'Agostino, L.Z., Kahn, H., Sant'Agostino, L.M., Tassinari, M.M.M.L. (Eds.), Applied Mineralogy, Developments in Science and Technology, vol. 2. ICAM-BR, São Paulo, pp. 781–784.

Ghavidel, M., 1973. Palynological Study of Well Finu No. 1 in Bandar Abbas Area, Geological Correlation with Kuh-e-Farag- han, Kuh-e-Gahkum and Well Namak #1. National Iranian Oil Company Report, Tehran, 60 pp.

Groves, I.M., Carman, C.E., 2003. Geology of the Beltana willemite deposit, Flinders Ranges, South Australia. Economic Geology 98, 797–818.

Hamdi, B., 1995. Precambrian–Cambrian deposits in Iran. In: Hushmandzadeh, A. (Ed.), Treatise of the Geology of Iran, vol. 20. GSI, 535 pp.

Hancock, M.C., Purvis, A.H., 1990. Lady Loretta silver–lead–zinc deposit. Geology of the mineral deposits of Australia and Papua New Guinea. Australasian Institute of Mining and Metallurgy 14, 943–948.

Heyl, A.V., Bozion, C.N., 1962. Oxidized zinc deposits of the United States, part I. General geology. U.S. Geological Survey Bulletin 1135-A, 52 pp.

Hirayama, K., 1968. Geological study on the Angouran mine, northwestern part of Iran. Geological Survey of Japan 226, 1–26.

Hitzman, M.H., Reynolds, N.A., Sangster, D.F., Allen, C.R., Carman, C.E., 2003. Classification, genesis, and exploration guides for nonsulphide zinc deposits. Economic Geology 98, 685–714.

Hitzman, M.W., 2001. Zinc oxide and zinc silicate deposits—a new look. Geological Society of America, Program with Abstracts 33, 1–336.

Hosseini-Dinani, H., Aftabi, A., 2015. Vertical lithogeochemical halos and zoning vectors at Goushfil Zn–Pb deposit, Irankuh district, southwestern Isfahan, Iran: implications for concealed ore exploration and genetic models. Ore Geology Reviews 72, 1004–1021.

Jacquat, O., Voegelin, A., Kretzschmar, R., 2009. Soil properties controlling Zn speciation and fractionation in contaminated soils. Geochimica et Cosmochimica Acta 73 (18), 5256–5272.

Large, D., 2001. The geology of nonsulphide zinc deposits—an overview. Erzmetall 54, 264–276.

Liaghat, S., Moore, F., Jami, M., 2000. The Kouh Sourmeh mineralization, a carbonate–hosted Zn–Pb deposit in the Simply Folded Belt of the Zagros Mountains, SW Iran. Mineralium Deposita 35, 72–78.

Lohmann, K.C., 1988. Geochemical patterns of meteoric diagenetic systems and their application to studies of paleokarst. In: James, N.P., Choquette, P.W. (Eds.), Paleokarst. Springer-Verlag, New York, pp. 58–80.

Majidifard, M.R., 1996. Stratigraphy, fossils and environment of Early Cretaceous rocks from the northern hills of Shirkuh. Geological Survey of Iran, Earth Science 20, 2–31 (in Farsi).

Maghfouri, S., Hosseinzadeh, M.R., Rajabi, A., Azimzadeh, A.M., Choulet, F., 2015. Geology and Origin of Mineralization in the Mehdiabad Zn-Pb-Ba (Cu) Deposit, Yazd Block, Central Iran, 13th SGA biennial meeting, Nancy-France.

Maghfouri, S., 2017. Geology, Geochemistry, Ore Controlling Parameters and Genesis of Early Cretaceous Carbonate-clastic Hosted Zn-Pb Deposits in Southern Yazd Basin, with Emphasis on Mehdiabad Deposit (Unpublished Ph.D. Thesis). Tabriz University, Iran, p. 475.

Momenzadeh, M., 1976. Stratabound Lead–Zinc Ores in the Early Cretaceous and Jurassic Sediments in the Malayer–Esfahan District (West Central Iran), Lithology, Metal Content, Zonation and Genesis (Unpublished Ph.D. Thesis). University of Heidelberg, Heidelberg, 300 p.

Monteiro, L.V.S., Bettencourt, J.S., Spiro, B., Graça, R., de Oliveira, T.L., 1999. The Vazante zinc mine, Minas Gerais, Brazil: constraints on willemitic mineralization and fluid evolution. Exploration Mining Geology 8, 21–42.

Moore, J.Mc M., 1972. Supergene mineral deposits and physiographic development in southwest Sardinia, Italy. Transactions Institution Mining and Metallurgy, Section B: Applied Earth Science 71, B59–B66.

Movahednia, M., 2014. The Geology of the Haft-har Deposit. Unpublished report.

Muller, D.W., 1972. The geology of the Beltana willemite deposits. Economic Geology 67, 1146–1167.

Nabavi, M., 1972a. Early Cretaceous Deposits in the Taft-Yazd and Khur area. Geological Survey of Iran, Report 106, pp. 1–127.

Nabavi, M.H., 1972b. Geological Quadrangle Map of Iran, H 9, Yazd 1:250,000. Geological Survey of Iran, Tehran.

Nosratian, J., 1991. Geological Map of Mehdi Abad. Based on the Topographical Map Mehdi Abad-Yazd, 1:2000.

Peck, W.P., Volkert, R.A., Mansur, A.T., Doverspike, B.A., 2009. Stable isotope and petrologic evidence for the origin of regional marble-hosted magnetite deposits and the zinc deposits at Franklin and Sterling Hill, New Jersey Highlands, United States. Economic Geology 104, 1037–1054.

Pride, K., Salehi, H., 2003. Angouran Zinc Deposit, Iran. Prospectors and Developers Association of Canada. Abstracts, 24.

Rajabi, A., Canet, C., Rastad, E., Alfonso, P., 2014. Basin evolution and stratigraphic correlation of sedimentary-exhalative Zn–Pb deposits of the Early Cambrian Zarigan–Chahmir Basin, Central Iran. Ore Geology Reviews 64, 328–353.

Rajabi, A., Rastad, E., Alfonso, P., Canet, C., 2012. Geology, ore facies and sulfur isotopes of the Koushk vent-proximal sedimentary-exhalative deposit, Posht-e-Badam block, Central Iran. International Geology Review 54, 1635–1648.

Rajabi, A., 2012. Ore Controlling Parameters and Genesis of Sedimentary-exhalative Zn-Pb (SEDEX Type) Deposits, Zarigan-Chahmir Area, East of Bafq, Central Iran (Unpublished Ph.D. Thesis). Tarbiat Modares University, Iran, p. 420.

Rastad, E., 1981. Geological, Mineralogical, and Facies Investigations on the Early Cretaceous Stratabound Zn–Pb–(Ba–Cu) Deposits of the Iran Kouh Mountain Range, Esfahan, West Central Iran (Unpublished Ph.D. Thesis). University of Heidelberg, Heidelberg, 334 p.

Reichert, J., 2009. A geochemical model of supergene carbonate-hosted nonsulphide zinc deposits. In: Titley, S.R. (Ed.), Supergene Environments, Processes, and Products, Society of Economic Geologists, Special Publication, vol. 14, pp. 69–76.

Reichert, J., Borg, G., 2008. Numerical simulation and a geochemical model of supergene carbonate-hosted nonsulphide zinc deposits. Ore Geology Reviews 33, 134–151.

Reichert, J., 2007. A Metallogenetic Model for Carbonatehosted Non-sulfide Zinc Deposits Based on Observations of Mehdi Abad and Iran Kouh, Central and Southwestern Iran (Unpublished Ph.D. Thesis). University of Martin Luther, Shillong, 129 p.

Reynolds, N., Large, D., 2010. Tethyan zinc–lead metallogeny in Europe, North Africa, and Asia. Society of Economic Geologists Special Publication 15, 339–365 pp.

Rose, A.W., Hawkes, H.E., Webb, J.S., 1979. Geochemistry in Mineral Exploration. Academic Press, London, 657 p.

Sangameshwar, S.R., Barnes, H.L., 1983. Supergene processes in zinc-lead-silver sulfide ores in carbonate rocks. Economic Geology 78, 1379–1397.

Santoro, L., Boni, M., Herrington, R., Clegg, A., 2013. The Hakkari nonsulfide Zn–Pb deposit in the context of other nonsulfide Zn–Pb deposits in the Tethyan Metallogenic Belt of Turkey. Ore Geology Reviews 53, 244–260.

Schlagintweit, F., Bucur, I.I., Rashidi, K., Hanifzadeh, R., Wilmsen, M., 2013a. Torremiroella hispanica Brun and Canérot, 1979 (benthic foraminifera) from the Early Cretaceous of Central Iran and its palaeobiogeographic significance. Cretaceous Research 46, 272–279.

Schlagintweit, F., Bucur, I.I., Rashidi, K., Saberzadeh, B., 2013b. Praeorbitolina claveli n. sp. (benthic foraminifera) from the Early Aptian (Bedoulian) of Central Iran. Carnets de Géologie/Notebooks on Geology, Letter 2013/04, pp. 255–272.

Slezak, P.R., Olivo, G.R., Oliveira, G.D., Dardenne, M.A., 2014. Geology, mineralogy, and geochemistry of the Vazante Northern Extension zinc silicate deposit, Minas Gerais, Brazil. Ore Geology Reviews 56, 234–257.

Solymani, B., 1996. Geochemistry, mineralogy and genesis studies of the Kuh-e-Surmeh lead-zinc deposit (MSc Thesis). Tarbiat Moallem University, Tehran, 250 pp. (in Persian).

Stara, P., Rizzo, R., Tanca, G.A., 1996. Iglesiente-Arburese, miniere e minerali. Ente Minerario Sardo I, 238 p.

Takahashi, T., 1960. Supergene alteration of zinc and lead deposits in limestone. Economic Geology 55, 1083–1115.

Wilmsen, M., Fürsich, F.T., Majidifard, J., 2013. The Shah Kuh Formation, a latest Barremian – early Aptian carbonate platform of Central Iran (Khur area, Yazd Block). Cretaceous Research 39, 183–194.

Williams, P.A., 1990. Oxide Zone Geochemistry. Ellis Horwood Ltd., Chichester, England, 286 p.

Zahedi, M., 1976. Explanatory Text of the Esfahan Quadrangle Map: 1:250,000; Geological Quadrangle F8. Geological Survey of Iran, 49 p.